Review Article

Current research trends and perspectives on materials-based hydrogen storage solutions: A critical review

Jianwei Ren [a,], Nicholas M. Musyoka [a], Henrietta W. Langmi [a], Mkhulu Mathe [a], Shijun Liao [b]*

[a] HySA Infrastructure Centre of Competence, Materials Science and Manufacturing, Council for Scientific and Industrial Research (CSIR), PO Box 395, Pretoria 0001, South Africa
[b] School of Chemistry and Chemical Engineering, South China University of Technology, Wushan Road, Tianhe District, Guangzhou 510640, China

ARTICLE INFO

ABSTRACT

Effective hydrogen storage solutions have been pursued for decades, and materials-based hydrogen storage is a research frontier of much current interest. Yet, no researched materials to date have come close to the DOE 2020 targets for hydrogen storage at ambient conditions, although some good results have been reported at cryogenic temperature. This paper critically reviews the current research trends and perspectives on materials-based hydrogen storage including both materials-based physical storage and materials-based chemical storage. In the case of physical storage, the efforts on exploring new porous materials with extra larger surface/pore volume, inducing hydrogen spillover effect, and tailoring reaction enthalpies are discussed. Meanwhile, for chemical storage, approaches to improve the kinetics and/or thermodynamics such as the development of composite hydride systems, nanoconfinement of hydride materials as well as the usage of ionic liquids as hydrogen storage materials or useful additives are discussed. Furthermore, the applied techniques on solid-state materials towards system integration such as shaping and electrospinning processes are introduced. Finally, the concept of storing hydrogen in para form for long-term hydrogen storage is discussed, and a converter packed with catalysts to process the normal hydrogen to para-hydrogen is highlighted.

© 2016 Hydrogen Energy Publications LLC. Published by Elsevier Ltd. All rights reserved.

Contents

Hydrogen as a fuel for the future

Today's world and particularly developing countries, rely heavily on fossil fuels. Most of the time, the fossil fuels are consumed for heat and electricity. The growing world population and increasing standard of life-style have led to a rapidly increasing demand of energy since 1950 and are projected to peak in 2035 (Fig. 1) [1]. Moreover, the non-renewable nature of fossil fuels such as coal, oil and natural gas at the humankind timescale has prompted governments in many
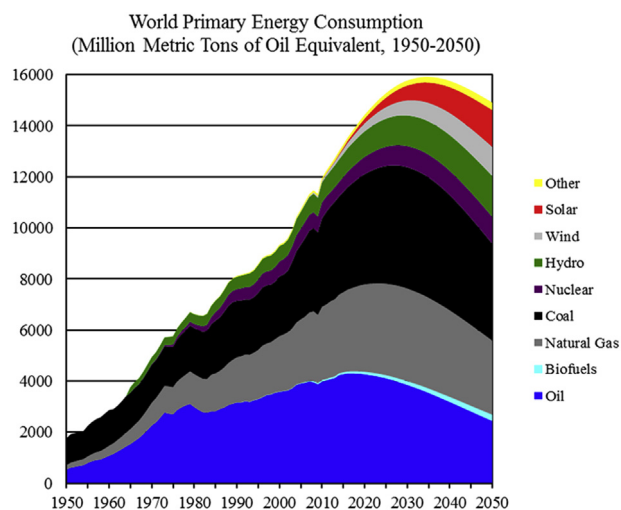

Fig. 1 − **World primary energy consumption. Re-produced from Ref. [1] with permission.**

countries to think about energy security. Fossil fuels will one day be inevitably used up, although this may not occur in the next two generations due to the relatively large reserves of natural gas and coal still available. However, with the current consumption rate the proven reserves of natural gas and coal should last for approximately 70 and 200 years, respectively, and oil is expected to deplete even earlier [2]. By that time, an alternative fuel is needed for the future energy demand when those fossil fuels become unavailable, more importantly for the transport sector, which is consuming almost 60% of the world energy [3]. Among potential candidates such as solar, wind, nuclear, tidal, hydro, biofuels and geothermal energy, hydrogen appears to be the best choice due to the highest energy density per unit mass (120 MJ/kg), no environmental implications and its abundance in the universe [4−6].

The proposed 'Hydrogen Economy' is driven by electricity, and hydrogen presents a means to store electricity via chemical bonds of hydrogen. Typically, 6 kg of hydrogen is able to allow a light-duty vehicle to run for 500 km [7]. Ideally, the amount of hydrogen should be carried as a small volume and light weight. For practicality, the 2020 targets set by the US DOE are: gravimetric capacity of 5.5 wt.% and volumetric capacity of 40 $g \cdot L^{-1}$ at an operating temperature of −40 to 60 °C under a maximum delivery pressure of 12 bar [8]. These values were described for a complete system including tank, materials, valves, regulators, piping, mounting brackets, insulation, added cooling capacity and other balance-of-plant components [8]. To date, the extensive utilization of hydrogen as a fuel is being hindered by lack of effective hydrogen storage solutions. At standard temperature and pressure with a low density of 0.089 $g \cdot L^{-1}$, 6 kg of hydrogen gas will occupy a

spherical volume of 5 m in diameter. Based on the PVT-characteristic, the common practice is to pressurize hydrogen gas into a steel cylinder. So far, high-pressure tanks have been rated to a maximum of 700 bar.

Despite such high pressures, as shown in Fig. 2 [9], at 700 bar, 6 kg of hydrogen still requires a storage tank with a volume of about 150 L. As another option, liquid hydrogen systems offer a higher density of 71 g·L^{-1} H_2 at −253 °C. But the heat input from the surroundings into the tank leads to the evaporation of the hydrogen, the so called boil-off phenomenon [10]. The currently available engineering technologies have not yet been able to prevent the heat input from the environment and suppress those losses [11]. These losses involve the conversion of para-hydrogen to ortho-hydrogen, which will be introduced in a later section. Therefore, purely pressurized and liquid H_2 are not considered as economically viable options for hydrogen storage.

Materials-based hydrogen storage systems

Recently, materials-based hydrogen storage has been considered as a long-term solution [12]. Considering both PVT-filling and adsorption effect, improved volumetric hydrogen storage capacities in materials-packed gas cylinders compared to cylinders without any materials can be expected. Depending on the type of materials, the storage system is based on either physical sorption (physisorption) as in the case of porous materials or chemical sorption (chemisorption) as in the case of metal/chemical hydrides. Physisorption involves weaker binding energy of 4−10 kJ·mol^{-1} and weak van der Waals forces, while chemisorption involves stronger binding energy of 50−100 kJ·mol^{-1} in complex hydrides and metal hydrides, where the hydrogen molecule is first

dissociated on the surface, followed by diffusion of the hydrogen atoms into the metal host lattice [13]. In comparison to chemisorption, physisorption processes are easy to handle, are reversible due to the low interaction energy, and possess fast adsorption−desorption kinetics [14]. In porous materials such as zeolites, porous carbon structures, and metal−organic frameworks (MOFs), hydrogen is physisorbed on the surface of the pores, and the capacity is mainly dependent on the surface area, pore volume, working pressure and working temperature. Typically, many of the physisorption based materials have acceptable hydrogen storage capacities at cryogenic temperatures (77 K) and high pressures, but their capacities drop to below 1 wt.% at ambient temperature and pressure in the range 50−100 bar [15]. Then the economic feasibility of storing hydrogen based on physisorption at cryogenic temperature becomes an issue that should also be addressed. Given the binding energy of hydrogen on the surface of a certain material is 10 kJ·mol^{-1} H_2, 6 kg H_2 will generate 30 MJ heat. If the 77 K temperature is maintained by liquid nitrogen with heat of vaporization of 5.6 kJ·mol^{-1}, then 5400 mol N_2 (150 kg) liquid nitrogen should be circulated around cylinder. Such large amount of liquid nitrogen for cooling purposes would lead to difficulties for the engineering work at a later stage. Usually for chemisorption with stronger binding energy, formation of hydrogen compounds occurs under elevated hydrogen pressure generating heat as a result of the exothermic reaction. In order to release the hydrogen, the pressure is reduced and heat is applied to the material. Although some metal hydrides can operate reversibly near ambient temperature, their gravimetric hydrogen storage capacities are lower than 3 wt.% [16]. Some light metal hydrides and complex hydrides possess high gravimetric storage capacities (e.g. 7.6 wt.% for MgH_2 and 18 wt.% for $LiBH_4$). However, releasing of hydrogen from these hydrides requires high

Physical Storage

| 1 bar normal 0.3 g/L | 150 bar lab cylinders 10 g/L | 350 bar Gen 1 vehicles 28 g/L | 700 bar Gen 2 vehicles 40g/L | liquid H_2 71 g H_2/L @ 20 K |

Materials-based Storage

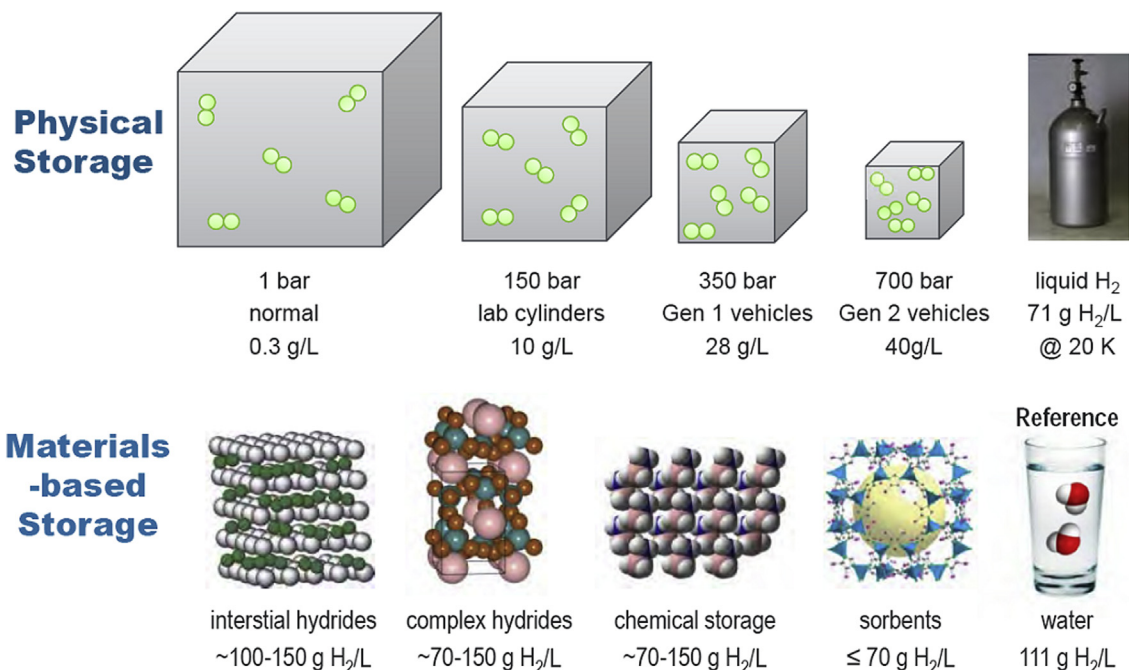| interstial hydrides ~100-150 g H_2/L | complex hydrides ~70-150 g H_2/L | chemical storage ~70-150 g H_2/L | sorbents ≤ 70 g H_2/L | Reference water 111 g H_2/L |

Fig. 2 − Compressed hydrogen vs. materials-based hydrogen storage [9]. Re-produced from Ref. [9] with permission. Copyright 2012.

temperatures. For instance, MgH_2 requires a temperature of about 573 K. Furthermore, the complex hydrides release hydrogen via multi-step reactions with different temperatures [17—20], which further complicates the heat management of the storage system. To enable hydrogen to be stored in a solid-state materials-based system at ambient temperature with acceptable storage density, different strategies have been investigated and evaluated. For porous materials-based physisorption systems, research is focused on improving hydrogen storage capacities at ambient temperature. For metal/chemical hydrides-based chemisorption systems, research is focused on improving kinetics and thermodynamics of the investigated materials as well as developing new materials and catalysts that will enable the achievement of high storage capacities at significantly lower temperatures.

Ionic liquids have been known since 1913, and their historical introduction together with recent progress has been reviewed by Wilkes [21] and Hajipour et al. [22], respectively. The established definition of ionic liquids is; salts in a liquid state with a melting point below 100 °C. The low melting points of ionic liquids result from the reduced lattice energy arising from the large ion-pairs and low symmetry of the cations [23,24]. Typically, they are composed of cations and anions which possess negligible vapour pressures, high densities, high thermal stabilities and are non-flammable [25]. Initially, ionic liquids were considered as green solvents for chemical synthesis, and their other properties have only emerged in the recent two decades [26]. Considering the widely accepted fact that liquid fuel system would offer more convenience to practical applications, ionic fluids have attracted interest as promoting agents for dehydrogenation and in some instances, for use in solubilisation of hydrogen carrier materials [27,28]. Stracke et al. [29] reported the potential of imidazolium ionic liquids for hydrogen storage, with a volumetric hydrogen capacity of up to 30 $g \cdot L^{-1}$ at atmospheric pressure, equivalent to twice that of compressed hydrogen gas at 350 bar. Nevertheless, the Pd/C-catalysed dehydrogenation temperature was in the range of 503—573 K, and a long hydrogenation time of 100 h was required in order to add more hydrogen atoms into the ionic liquid. Even though this performance did not specifically lead to a breakthrough, it is worth pursuing the research topic further in order to draw a meaningful conclusion on the appropriateness of this exciting class of materials for hydrogen storage applications [30]. The research trends on ionic liquids will be discussed in Section Research trends on ionic liquids for hydrogen storage applications.

Research trends on porous materials-based physical sorption

There is increasing potential to achieve reliable hydrogen storage capacities in porous materials-based systems [11—14,17,31]. Of the existing porous materials, metal-organic frameworks (MOFs) and porous carbonaceous materials have been identified to be attractive for hydrogen storage [11,14,31—33]. Some studies [34,35] have also highlighted the enhancement of hydrogen storage capacities, thermostability and hydro-stability that can be achieved on porous

hybrid composites of MOFs and carbon materials. Up to date, most research strategies are being focused on ways of achieving better performance of porous materials-based physical sorption at ambient temperature, and several comprehensive reviews have covered some of these studies in detail [36—41].

Exploration of new materials with higher Brunauer—Emmett—Teller (BET) surface areas and larger pore volumes

It is generally believed that higher BET surface areas and larger pore volumes will enhance hydrogen storage capacities [31,32]. Carbon aerogel [42] and MOF-210 [43] materials have BET surface areas of 3200 and 6240 $m^2 \cdot g^{-1}$, respectively. Nu-109 and NU-100 materials [44] exhibit the highest experimental BET surface areas of any porous materials (~7000 $m^2 \cdot g^{-1}$) reported to date. However, Suh et al. [45] indicated that the H_2 uptake capacities at 77 K and 1 bar only correlate with the BET surface areas below 2000 $m^2 \cdot g^{-1}$, and are no longer applicable when the BET surface area exceeds 2000 $m^2 \cdot g^{-1}$ (Fig. 3). The argument was that, at 77 K and 1 bar of H_2 pressure, H_2 molecules cannot completely cover the surface area larger than 2000 $m^2 \cdot g^{-1}$ because at low pressure, H_2 prefers to bind on the sites with large affinity for H_2. This conclusion was supported by the Grand Canonical Monte Carlo (GCMC) simulations [45], and the results showed the occurrence of three adsorption regimes as follows: in the low pressure region, H_2 uptake relates to the heat of H_2 adsorption, while at intermediate pressure (up to 30 bar) it correlates with the surface area, and at high pressures (120 bar) with the free volume (Fig. 4).

Given the fact that at ambient temperature the surface coverage of a material by H_2 molecules is much lower than that at 77 K, for a material with a BET surface area larger than 2000 $m^2 \cdot g^{-1}$, the enhancement of hydrogen storage capacities
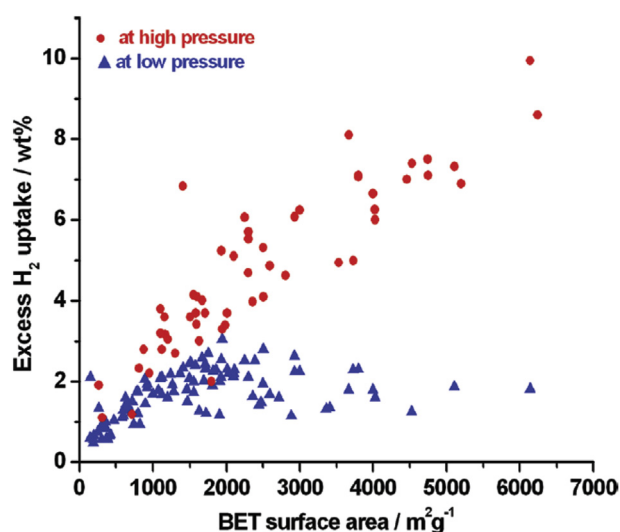

Fig. 3 — A plot showing the relationship between H_2 uptake capacities at 77 K and BET surface areas of various MOFs. Low pressure is 1 bar and high pressures are in the range of 10—90 bar. Re-produced from Ref. [45] with permission. Copyright 2012 the American Chemical Society.
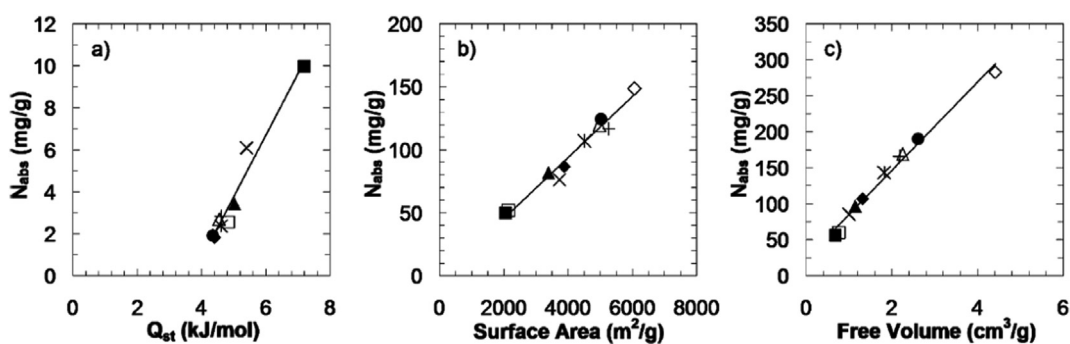
Fig. 4 — (a) Amount adsorbed at 0.1 bar vs isosteric heat of adsorption. (b) Amount adsorbed at 30 bar vs accessible surface area. (c) Amount adsorbed at 120 bar vs free volume. ◆, IRMOF-1; ■, IRMOF-4; ▲, IRMOF-6; ×, IRMOF-7; *, IRMOF-8; ●, IRMOF-10; +, IRMOF-12; △, IRMOF-14; ◇, IRMOF-16; □, IRMOF-18. Re-produced from Ref. [46] with permission. Copyright 2006 the American Chemical Society.

due to further increase in BET surface area above 2000 $m^2 \cdot g^{-1}$ will be significantly limited. It is therefore not advisable to put too much effort in pursuit of new materials with extra large surface areas only since H_2 adsorption may be influenced by a range of other factors. For example, in the case of MOFs, H_2 adsorption is also influenced by pore size, open metal sites, ligand functionalization, and catenation [47,48].

Tailoring reaction enthalpies

Out of the ongoing development of new materials and concepts [49–53], enthalpy of adsorption has drawn extensive attention from the hydrogen storage research community. For a developed material for hydrogen storage purpose, if this value is too high as in the case of chemisorption materials, large amounts of heat will be released during the charging process, and extra energy will be needed to enable the release of hydrogen for applications. In contrast, for physisorption materials, the enthalpy of adsorption is too low and thus, low hydrogen storage capacities can be expected at ambient temperature and pressure. To achieve high storage capacities, cryogenic temperature is required to maintain high density of hydrogen molecules on the material. Porous materials like MOFs and carbons usually exhibit very large surface areas and high hydrogen storage capacities at cryogenic temperature. However, at ambient temperature the storage capacities of these materials are low because the adsorption enthalpy is low implying the materials cannot effectively bind hydrogen on the surface under this at such temperatures. For instance, over 60 carbon materials were studied under ambient conditions, and the reversible storage capacities ranged between 0.04 and 0.46 wt.% [54,55]. To date, none of the developed MOF materials meets the US DOE 2020 hydrogen storage capacity target of 5.5 wt.% at the system-level at moderate temperature and pressure. The key setback is the weak van der Waals forces between H_2 molecules and the pore surface of MOFs. Similarly to carbon materials, although some MOFs with large surface area and pore volume can reach values not far from the target at cryogenic temperatures, those values fall to below one-tenth of the cryogenic values at moderate temperature. As discussed in Section 3.1, the H_2 storage capacities of MOF materials at 77 K and high pressure can be associated

with the free volume. Since the common practice is to store hydrogen in a steel bottle at a pressure of about 150 bar at 298 K, understanding the relationship between the heat of H_2 adsorption and hydrogen storage capacities under such condition is important. The reported data from literature were collected and plotted into Fig. 5 by Suh et al. [45].

As seen in Fig. 5, the H_2 heat of adsorption values for most of the MOFs are in the range of 4–12 $kJ \cdot mol^{-1}$. As the value increases from 4 to 12 $kJ \cdot mol^{-1}$, the high pressure H_2 storage capacities at 77 K were not improved to a large extent (Fig. 5a). Nevertheless, at 298 K and 10–90 bar, the H_2 storage capacities generally seemed to increase with increased heat of adsorption (Fig. 5b). Given a H_2 adsorption enthalpy of 6 $kJ \cdot mol^{-1}$, as calculated by Bhatia et al. [56], the optimal operating temperature is 131 K between 1.5 and 100 bar. It is thus necessary to increase the binding ability of H_2 to MOF materials in order to avoid the use of costly and cumbersome cooling system. In this regard, several strategies have been explored, for instance, Kubas binding, ionization, polarization and irradiation of the host materials.

Usage of Kubas binding
As discussed in the previous section, the low heats of adsorption in the range of 4–10 $kJ \cdot mol^{-1}$ based on H_2 physisorption are too weak to hold hydrogen molecules on to the surface of the material, leading to low hydrogen storage capacities. On the other hand, binding enthalpies of 40–100 $kJ \cdot mol^{-1}$ based on H_2 chemisorption are too strong to allow hydrogen to be released easily, resulting in poor reversibility and slow kinetics. As such the energy storage capacity of the developed system in reality reduces considerably with the complicated heat management. Some reports have indicated that a binding enthalpy of 20–30 $kJ \cdot mol^{-1}$ is ideally required to operate a hydrogen storage system at room temperature [57–59]. Such binding enthalpy values allow for a sufficiently strong interaction between hydrogen and the material as well as provide less problematic heat management [60]. In order to achieve the desired binding enthalpy exploration of Kubas interaction has been suggested [61–64]. Kubas interaction involves σ donation from the filled σ-bonding orbital of H_2 molecule to an unfilled d orbital of a transition metal, and at the same time π back-donation from a
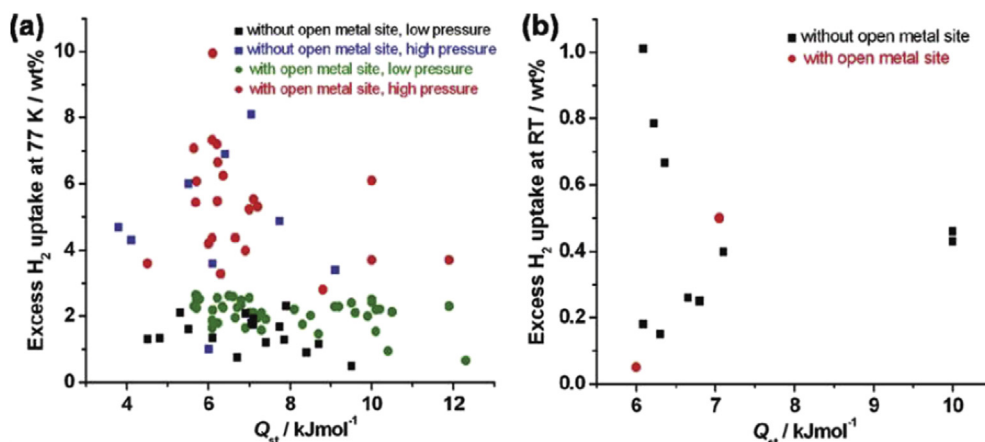
Fig. 5 — A plot showing the relationship between high pressure H₂ uptake capacities in excess and Qst of the H₂ adsorption. (a) At 77 K. (b) At 298 K. Low pressure is 1 bar, and high pressures are in the range of 10–90 bar. Re-produced from Ref. [45] with permission. Copyright 2006 the American Chemical Society.

filled d orbital of a transition metal to the empty σ* anti-bonding orbital of the H₂ molecule. In terms of binding strength (see Fig. 6), Kubas interaction is at the mid-point of physisorption and chemisorption, thus this concept can be potentially employed in hydrogen storage systems designed to operate at room temperature [65]. Several studies [66–70] have demonstrated that Kubas interaction can be exploited in designing novel hydrogen storage materials that eliminate the limitations arising from physisorption and chemisorption mechanisms.

Ionization of the host materials
Another alternative strategy for designing materials with improved performance of H₂ storage follows on from the concept of Kubas interaction discussed above. Based on Kubas interaction, many transition metal complexes have been studied as potential hydrogen storage materials [52,71–79]. A new approach emerging from this concept has been proposed by several research groups. Stefanakos et al. [80] believed that ionization of the host materials and hydrogen molecules could lead to enhancement of hydrogen

adsorption. In the latter case, they used modified fullerene (with Na⁺ and K⁺ as dopants), and demonstrated that the hydrogen adsorption capacity can be raised from 2.8 wt.% to 3.1 wt.%. Liu et al. [81] illustrated that charged $Li_2C_2H_4$ and TiC_4H_4 complexes improve the metal bond strength as well as increase the number of non-dissociative H₂ molecules attached. Guo et al. [82] employed $C_4H_4^+$ as substrate for Co and Ni atoms, and attributed the enhancement in hydrogen storage capacity from 3.48 to 5.13 wt.% for the CoC_4H_4 complex, to the ionic processes involved. Wang et al. [83] studied Li_2F coated C_{60}, and the resulting gravimetric and volumetric H₂ storage densities for $C_{60}(Li_2F)_{12}$ were 10.86 wt.% and 59 g·L⁻¹, respectively, obtained through calculations. The binding energy of dihydrogen is within the expected range, which enables hydrogen sorption/desorption to occur at ambient conditions.

Polarization of the host materials
Yaghi et al. [84] proposed a structure polarization strategy for further improvement of hydrogen storage in MOFs. Using density functional theory, Yoon et al. [85] conducted a
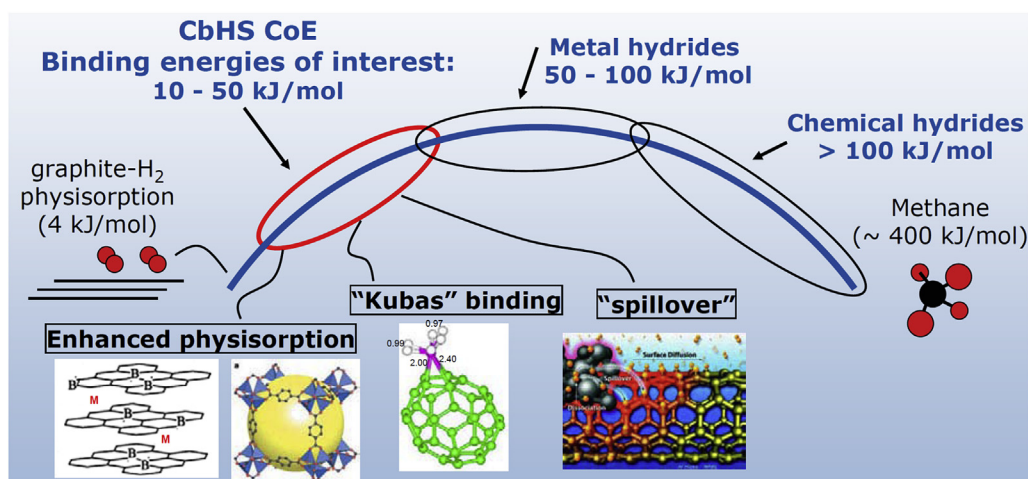

Fig. 6 — Re-produced from Ref. [57] with permission.

systematic study on how charging of carbon fullerenes can affect their ability to bind hydrogen molecules. It was reported that the binding strength of molecular hydrogen on either positively or negatively charged fullerenes can be remarkably improved to the desirable range for possible application at room or near ambient temperature. The enhanced binding is associated with the polarization of the hydrogen molecules by the high electric field that is created near the surface of the charged fullerene, and is delocalized, surrounding the entire surface of a charged fullerene. Zhou et al. [86] directly applied an external electric field to hydrogen storage nanomaterials. Using density functional theory, they demonstrated that in an applied electric field polarization of the electrons of the hydrogen molecules occurs, and the electrostatic interactions between the hydrogen molecules and the substrates enhance the storage performance considerably. Even more significant is the fact that upon removal of the applied electric field, the system returns to its original state and hydrogen molecules simply desorb, resulting in good reversibility and fast kinetics. The study suggested that this approach of directly applying an external electric field would lead to a simpler synthesis of materials while enhancing the thermodynamics and reversibility of hydrogen storage. It was also noted that the storage of hydrogen in quasi-molecular form by exposed metal cations occurred via a polarization mechanism where the H_2 molecule is polarised by the electric field associated with point ions [86,87].

Irradiation of the host materials

The concept of irradiation was proposed by Muga et al. [88] to alter the reaction behaviour of host storage materials with hydrogen thereby improving their hydrogen storage capacity. Such alteration involves adjustment of the electronic configuration of the storage material. According to their report, penetrating radiation can excite and activate the electronic environment at surface as well as interior sites, making the sites ready for bonding with hydrogen in a quasi-manner. This mechanism is supported by other researchers [89]. Obolensky et al. [90] reported increased (~15%) hydrogen sorption/desorption capability for carbon nanotubes following irradiation by γ-rays. Novaković et al. [91] examined the effects of well-defined structural changes introduced within a thin surface layer of MgH_2 as a result of irradiation with Xe ions, and found that it is possible to control the thermodynamic parameters by controlled ion bombardment.

Inducing the H_2 spillover effect

For practical purposes, porous materials are expected to adsorb/release H_2 efficiently near room temperature. A concept of storing hydrogen in porous materials based on the 'spillover' mechanism has been proposed and evaluated. Generally, it involves loading of a metal catalyst such as Pd, Pt, Ni on the porous materials as hydrogen dissociation catalyst to create atomic hydrogen (Fig. 7) [92]. The dissociated H atoms migrate from metal particles to the support material with a lower activation energy (<10 kJ·mol^{-1}), and the adsorbed hydrogen migration can occur reversibly from the support surface back to metal particle surface for desorption [93]. One of the most appealing features of such concept is the possibility to operate the hydrogen storage system at room temperature rather than cryogenic temperature (77 K) [93].

In order to make the system suitable for room temperature operation, many post-synthetic strategies for porous materials to induce hydrogen 'spillover' have been evaluated. So far, this technique has been experimentally demonstrated by over 600 publications from more than 70 research groups globally, as reviewed by several groups [93—97]. Some studies have reported enhancement of hydrogen storage capacity in MOFs by using metals (such as Pt, Pd, Ru and Ni) together with a support composed of high surface area material (such as activated carbon) to promote the hydrogen 'spillover' effect [98—107]. In addition, some theoretical studies have been conducted to explain hydrogen spillover in MOF materials [34,108—116]. However, despite these positive reports, there are some experimental studies that have discredited hydrogen storage by spillover effect, and reported the attained spillover enhancement factors to be smaller than 8, if not below the detection limit [117—120]. To date, the understanding of spillover for hydrogen storage is limited. As highlighted by Prins [86], spillover does not occur in all circumstances, and caution must be exercised before attributing a scientific occurrence to spillover. It is generally believed that the mechanism involved in carbon hydrogenation i.e. when hydrogen atoms are chemisorbed, is the transition from sp^2 to sp^3 hybridization [121]. Also during our review of the literature, we noticed that in most of the cases, spillover was reported to occur in the presence of carbon materials. In other words, carbon materials and H atoms are able to bind exothermally, but in the case of MOFs, it is unclear how the binding between H atoms and for example, organic units in the MOFs, would take place. For instance, the spillover on MIL-101 was not evidenced even by careful and complex experiments [122]. The research regarding 'spillover' effect is still ongoing [123—128], although inaccurate measurements have created confusion in the research community, and no independent groups have succeeded in reproducing the enhanced storage. Tsao group [129] claimed that oxygen content and functional groups on the surface of support accounted for the room temperature enhanced hydrogen storage capacities. Razzhivina et al. [130] recently observed hydrogen spillover through a gas phase in a 5% Pd/C catalyst-sodium 4-phenylbenzoate system employing tritium as a tracer. From our view to date, plenty of time and funds were invested from research groups by trying to replicate results.

Research trends on metal/chemical hydrides-based chemical sorption

The term 'metal hydride' referred here encompasses conventional hydrides such as Mg_2NiH_4 and $LaNi_5H_6$, and complex hydrides such as borohydrides, alanates and amides. Among the metal hydrides, light-weight hydrides such as MgH_2 and $LiBH_4$ have received immense interest because of their high hydrogen storage densities, both gravimetrically and volumetrically. As known, in general, shortcomings of metal/chemical hydrides for hydrogen storage practices are sluggish kinetics of hydrogen desorption/absorption,
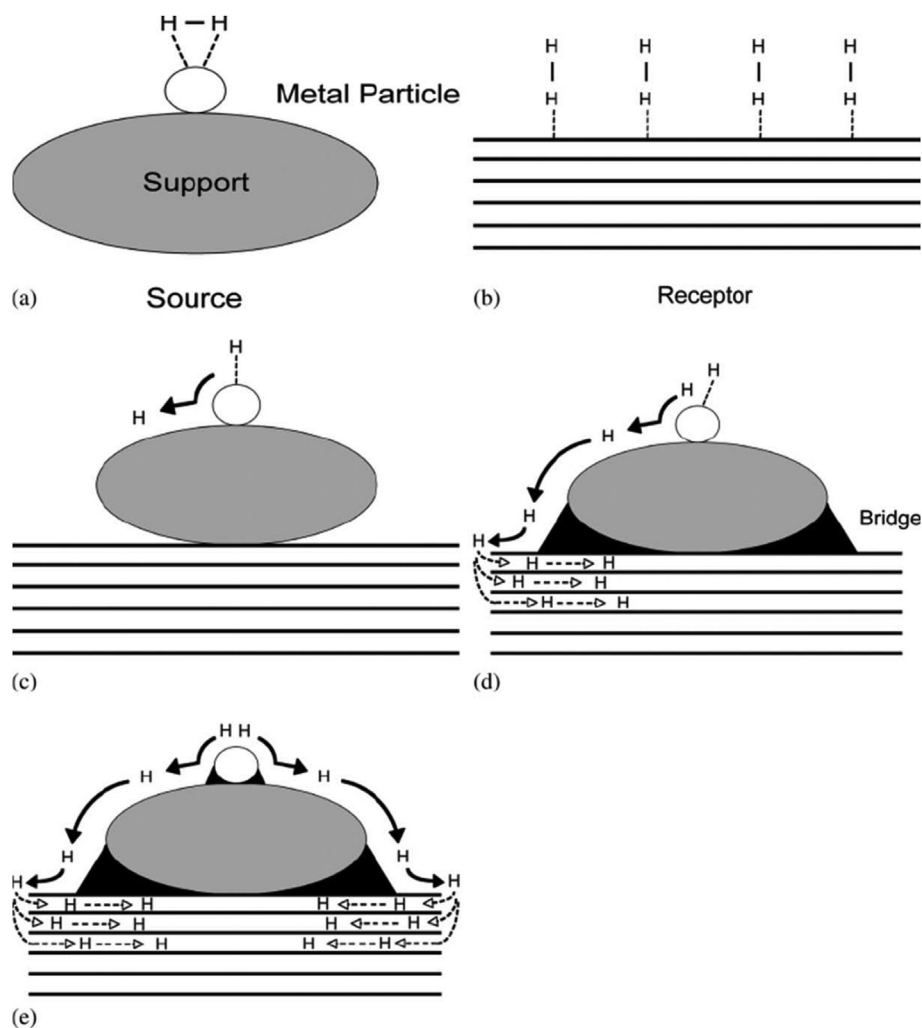
Fig. 7 – Hydrogen spillover in a supported catalyst system: (a) adsorption of hydrogen on a supported metal particle; (b) the low-capacity receptor; (c) primary spillover of atomic hydrogen to the support; (d) secondary spillover to the receptor enhanced by a physical bridge; (e) primary and secondary spillover enhancement by improved contacts and bridges. Reproduced from Ref. [93] with permission. Copyright 2005 the American Chemical Society.

relatively high thermal stability, irreversible hydrogen storage and unwanted side gases. In the following subsections, we highlight several strategies towards enhancing the hydrogen storage characteristics of metal hydrides. Particular attention is given to those strategies geared towards lowering the operating temperature, enhancing the uptake/release kinetics and suppressing the formation of unwanted gases during desorption. These and several other approaches have also been reviewed elsewhere [11,49,50,131–134].

Development of reactive hydride composites

Two or more reactive hydrides can be mixed together to form a reactive hydride composite. In such systems, the overall reaction enthalpy is lowered as a result of the formation of a new product through an exothermic reaction while releasing hydrogen through an endothermic reaction of the constituent hydrides. Consider the composite system composed of $LiBH_4$ and MgH_2, the theoretical hydrogen storage capacities of the individual hydrides are 18.5 and 7.6 wt.%, respectively and

their enthalpies are −70 and −75 $kJ \cdot mol^{-1}$ H_2, respectively. This implies the constituent hydrides must be heated to high temperatures to release hydrogen. MgH_2 alone needs to be heated to 300 °C for desorption of hydrogen at 1 bar, while temperatures in excess of 400 °C are necessary for complete release of hydrogen from $LiBH_4$, and even more extreme conditions are required for its rehydrogenation. On the other hand, the composite system can release 11.4 wt.% H_2 in a single step with a much lower reaction enthalpy of −45 $kJ \cdot mol^{-1}$ H_2, forming MgB_2, and as such ensuring the thermodynamic feasibility of the reversible hydrogen uptake [135]. Recently, He et al. [136] synthesized borohydride hydrazinates (e.g. $LiBH_4.NH_2NH_2$ and $LiBH_4 \cdot 2NH_2NH_2$) by coordinating NH_2NH_2 with $LiBH_4$ as new hydrogen storage materials. They found 13 wt.% H_2 can be released from $LiBH_4 \cdot NH_2NH_2$ at 140 °C in the presence of Fe-B catalysts. Luo et al. [137] synthesized a new complex of $LiBH_4 \cdot NH_3BH_3$ by mechanically milling NH_3BH_3 and $LiBH_4$ in equivalent molar ratio. The resulting mixture released 15.7 wt.% hydrogen upon heating to 450 °C. Shin et al. [138] demonstrated the

incorporation of hydrolysable BH_4^- into the clathrate hydrate to form a hybrid hydrogen storage material tetra-n-butylammonium borohydride [(n-C_4H_9)$_4$NBH$_4$]. Other new perspectives of complex hydrides for hydrogen storage were reviewed by Ley et al. [139] about nanoporous hydride, anion substitution, and multi-functional metal borohydrides. In summary, reactive metal hydride composites could pave the way for new developments in the metal/chemical hydride research space, but it must be realised that although some of these materials are conceptually fascinating their applicability in real hydrogen storage systems are yet to be realised.

Nanoconfinement of hydride materials

Although some hydride materials (such as LiBH$_4$ and MgH$_2$) have high theoretical energy densities, their thermodynamics and kinetics are unfavourable for hydrogen storage practices under moderate pressure and temperature conditions. Finding a way to improve these properties is essential. Nanoconfinement is one of the important material processing techniques to enhance the thermodynamics and kinetics of those hydrides in hydrogen charging/discharging cycles. The strategy here is to achieve much higher reaction surfaces in a manner of decreasing the sizes of the hydride particles. Given a reaction of metal M with hydrogen to form a binary hydride MH_2 in Eq. (1), the molar free energy involved in the process can be obtained from Eq. (2) [140,141].

$$M + H_2 \leftrightarrow MH_2 \tag{1}$$

$$\Delta G(r) = \Delta G_0(r) + RT \ln\left(\frac{\alpha_{MH_2}}{\alpha_M P_{H_2}}\right) + \frac{3V_M E_{M \to MH_2(\gamma,r)}}{r} \tag{2}$$

where V_M is the molar volume, r is the particle radius, α is the chemical activity, and γ is the surface free energy or surface tension. $E_{M \to MH_2(\gamma,r)}$ is the surface energy, as expressed in E_{ads} (3). The factors involved are the surface free energies, particle radius, molar volumes and the adsorption energies of both the metal and the resultant metal hydride.

$$E_{M \to MH_2(\gamma,r)} = \left[\gamma_{MH_2}(r)\left(\frac{V_{MH_2}}{V_M}\right)^{2/3} - \gamma_M(r)\right] + E_{ads} \tag{3}$$

As shown in Fig. 8, the primary process of nanoconfinement involves finding a nanoporous material with preferably uniform pore sizes, which can be used as a scaffold, and then confining the hydride materials into those pores [142]. In such a way, the particle growth and agglomeration of the hydrides would be limited to the pore sizes of the scaffold, resulting in 'confined' particle sizes. Compared to other techniques such as high-energy ball milling, this is a more direct preparation of hybrid composites with the loading of small-sized hydride particles. Nanoconfinement of various hydrides (such as ammonia borane and dimethylamine borane) in a carbon or MOF material has been investigated both theoretically and experimentally, and the modelling predictions were in agreement with the experimental results. Importantly, the theoretical calculations also indicated that effects of particle sizes on the thermodynamic properties can only be envisaged when particle sizes are smaller than 2–3 nm [143–146]. In recent years, the technique of nanoconfinement has been
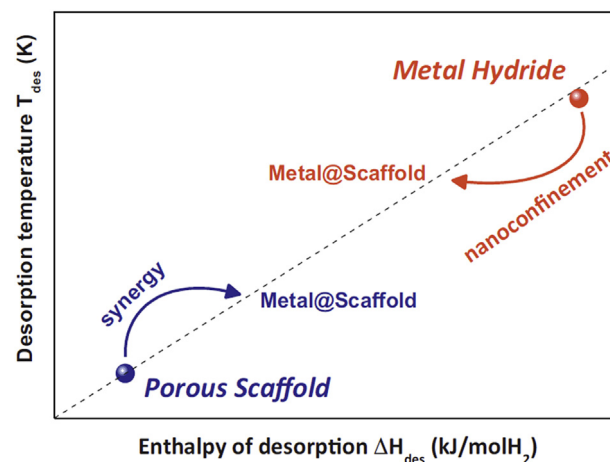

Fig. 8 – Tailoring the enthalpies of both H$_2$ physisorption on porous scaffolds and hydrogen desorption from metal hydride by using a metal@scaffold hybrid. Re-produced from Ref. [142] with permission. Copyright 2005 Elsevier.

employed on hydrides to modify their thermodynamics, aiming for the reversible hydrogen storage in practice (Table 1) [147–176]. Melt infiltration, as one of the routes to nanoconfinement, introduces nanoparticles of hydrides into a nanoporous scaffold material. This presents several benefits in terms of material's properties including enhanced surface area, more grain boundaries and diffusion distances in the nanoscale, which lead to improved hydrogen desorption/absorption kinetics.

This concept to nanoconfine chemical reactions has been well elaborated in several review papers [177–180]. As a new piece of nanoconfined chemistry, it has been recognized as an important technique in the field of nanotechnology to improve or modify the profiles of chemical reactions. For hydrogen storage purpose, more implementation of this technique is expected in the near future.

Synthesis of new generation light-weight composite structures

Another thought is that the employment of light-weight hybrid hydrides has the potential to achieve better performance for hydrogen storage. To synthesize the light-weight compounds, the choice of elements should come from the elements with atomic number below 20. As known, the majority of compounds from this category are intrinsically very air/moisture sensitive, and as a result the induced degradation is a critical issue that needs to be addressed.

Recently, a breakthrough research gave new expectations to overcome this problem [181]. The authors embedded the air sensitive magnesium hydride in a gas selective polymer matrix called polymethyl acrylate (PMMA). The pictorial representation is shown in Fig. 9. Since the embedded hydride was prepared in the order of quantum dots, the reactive and fast reaction kinetics was claimed on the resulting composite. Such thinking could be applied to other high capacity hydride materials with thermo-dynamical shortcomings.

Table 1 – Nanoconfinement of hydride materials in different scaffolds[147–176].

Hydride	Scaffolds	Reference	Hydride	Scaffolds	Reference
AB[*]	JUC-32-Y	[147]	$LiBH_4/LiAlH_4$	Nanoporous graphite	[162]
AB[*]	Mg-MOF-74	[148]	$LiBH_4$-MgH_2-$NaAlH_4$	Nanoporous carbon	[163]
AB[*]	Zn-MOF-74	[149]	$Ti(BH_4)_3$	MOF	[164]
AB[*]	MIL-101, Ni@MIL-101	[150]	$LiBH_4$-$Ca(BH_4)_2$	Carbon aerogel	[165]
AB[*]	MIL-101, Pt@MIL-101	[151]	$LiBH_4$-Mg_2NiH_4	mesoporous carbons	[166]
AB[*]	ZIF-8	[152]	$LiBH_4$	Densified zeolite-templated carbon	[167]
DMAB[*]	ZIF-8	[153]	$LiBH_4$	Activated carbon	[168]
$NaAlH_4$	Ti@Mg-MOF-74	[154]	$NaBH_4$	graphene	[169]
$NaAlH_4$	HKUST-1	[155]	$Li_2Mg(NH)_2$	Thin-film hollow carbon spheres	[170]
$NaAlH_4$	MIL-125(Ti)	[156]	AB[*]	UiO-66	[171]
$LiBH_4$	HKUST-1	[157]	$Mg(BH_4)_2 \cdot 6NH_3$	Activated carbon	[172]
$LiBH_4$	MC-NbF₅	[158]	AB[*]	Polypyrrole nanotubes	[173]
$LiBH_4$	Activated carbon	[159]	$Mg(BH_4)_2$	Carbon nanotubes	[174]
$LiBH_4$	Ni@C	[153]	MgH_2 nanoparticles	Microporous carbon	[175]
$2LiBH_4$-MgH_2	ZrCl₄@Carbon aerogel	[160]	$LiBH_4$	Modified carbon nanotubes	[176]
$LiBH_4$	Activated carbon nanofiber	[161]			

[*] AB: ammonia borane (NH_3BH_3); DMAB: dimethylamine borane ($H_3B \cdot NMe_2H$).

Research trends on ionic liquids for hydrogen storage applications

Ionic liquids as hydrogen storage materials

The unique physico-chemical properties of ionic liquids make them attractive for hydrogen storage applications. The simplest idea is to find a low molecular weight but hydrogen rich ionic liquid that can serve as a hydrogen storage material. Furthermore, the H_2 release rate, operating temperature and H_2 purity are other key criteria that have stimulated intense research efforts towards development of new ionic liquid compounds with improved hydrogen storage performance [29,182]. For instance, an ionic liquid of methyl-guanidinium borohydride $[N_3H_8C]C^+BH_4$ was reported by Doroodian et al. [183] to release 9.0 wt.% H_2 under both thermal and catalytic conditions. The combination of guanidinium cation and the octahydrotriborate anion was reported to yield guanidinium octahydrotriborate with a H_2 storage capacity of 13.8 wt.% [184]. An N-substituted amine-borane ionic liquid was also synthesized in good yield using silyl
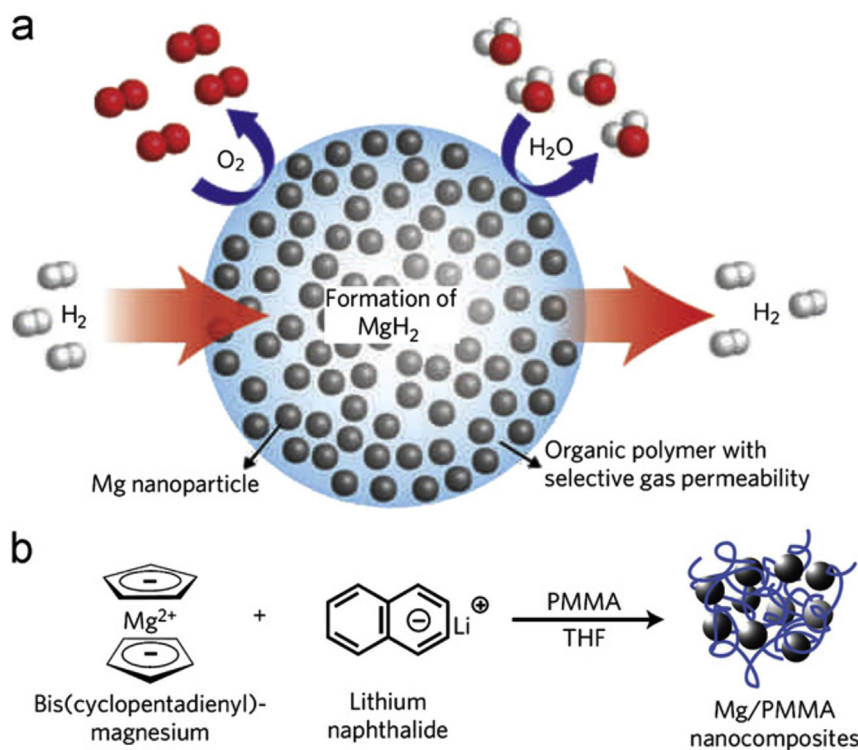

Fig. 9 – Pictorial representation of hydrogen permeation through MgH_2 nanoparticles buried inside PMMA gas selective polymer. Re-produced from Ref. [181] with permission. Copyright 2011 nature publishing group.

protecting groups and was found to generate a highly pure (1% impurity) H_2 gas [185].

Ionic liquids as catalytic or supporting solvents

Since the catalytic effects of ionic liquids were observed and discussed [186,187], the enhancement of hydrogen release and suppression of induction time on hydride-based H_2 storage system can be expected when ionic liquids are added [188]. It is also generally accepted that a mixture of selected chemical hydrides and ionic liquids would achieve synergistic effects [189–191]. While ionic liquids (as green solvents) afford an inert reaction medium which stabilizes polar transition states and substantially fastens the decomposition of chemical hydrides, the catalytic effects from the used ionic liquids also favour the H_2 release rate. In the decomposition of formic acid, studies were conducted by employing amine-functionalized imidazolium-ionic liquid [192–194], and it was found that it enabled better control of the equilibrium of formic acid with H_2/CO_2 [195]. Some other studies have also proved that ionic liquids can act as supporting solvents which enable improved performance, such as when heteronuclear Au–Pd nanoparticles are immobilized in the functionalized ionic liquid [C$_2$OHmim][NTf$_2$] [196].

Owing to the unique solubilization properties together with supporting effects in dehydrogenation reactions, ionic liquids have been ear-marked as promising contenders for hydrogen storage and also as valuable additives to hydrogen storage systems. Compared to the currently available compressed or cryogenic hydrogen storage options, the advantage of storing hydrogen in ionic liquids or their integrated systems is that the system does not require compression or cryogenic temperatures. However, for ionic liquid to be practically applicable issues related to their high cost of decomposition reaction and the compromised gravimetric capacity by the weight addition of ionic liquids to the H_2 storage system would need to be addressed. From the review of Prechtl et al. [197], the latter drawback has been claimed to be fully compensable in some cases since the ionic liquids-based systems gave much higher hydrogen yields in shorter reaction times than the dehydrogenation of neat hydrogen-rich materials.

Processing of solid-state materials towards system integration

No matter what mechanism the selected material works on, if the material is in the form of loose powder, it is necessary to process such powder material before the system integration for hydrogen storage applications. Given a material-based hydrogen storage unit, both exothermic and endothermic reactions are involved during a charging/discharging cycle. To allow a hydrogen storage unit based on solid-state materials quickly reach the desired equilibrium within maximum hydrogen input and shorter refuelling time, the heat generated during adsorption from the material bed should be dissipated effectively to avoid a temperature rise in the material bed [198,199]. The powder morphologies are usually not favourable for efficient thermal transport, which poses an issue on the system design [200,201]. In a charging process, the

heat of hydrogen adsorption on material beds, compression work and thermal mass from the inlet hydrogen gas are the main sources of heat generation. In the case of metal hydride beds, a noticeable temperature rise/drop can be expected in the charging/discharging cycle. The common solution is to integrate a heat-exchanger, which undoubtedly will compromise the performance from a system-level [202]. Two types of techniques that have been employed in the processing/shaping of solid-state materials towards improving thermal conductivity and system integration for hydrogen storage are discussed below.
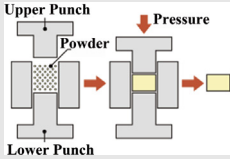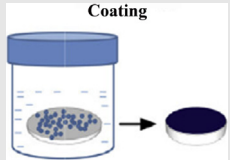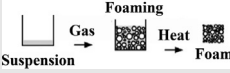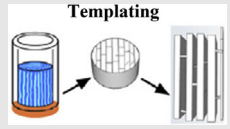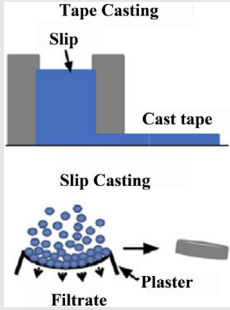
Powder shaping techniques

In order to improve thermal conductivity, powder materials are shaped into application-oriented structures such as beads, pellets or monoliths, and that enables the materials to pack uniformly. Shaping helps to maximize the bulk density, reduce wasted space in the storage container and resist attrition [203]. For practicality, expanded natural graphite (ENG) with high stability and thermal conductivity has been proved to be effective as a heat transfer matrix [204]. For example, addition of 10 wt% ENG and densification to 0.5 g/cm^3 led to the enhancement of thermal conductivity from 0.10 to 0.56 W/mK for MOF-5/ENG composite at room temperature [205,206]. Various processing routes for porous materials, as listed in Table 2 including foaming, coating, templating, slip casting, granulation, tape casting, extrusion, pulsed current processing, mechanical/hydraulic pressing, and testing techniques for shaped structures have been reviewed by several groups [207–209].
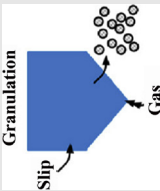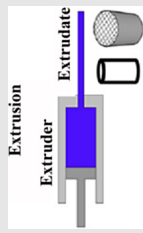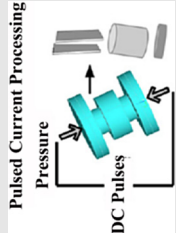
In order to choose a shaping technique, the preparation method and textural properties as well as other properties of the chosen powder material such as moisture sensitive, thermal stability and chemical stability should be taken into account. Also, for general applications, an appropriate mechanical strength is necessary to ensure low abrasion in packed beds. In addition, a low flow resistance is expected to guarantee a low-pressure drop. Finally, it is essential that the shaping process is cost effective and not complex as well.

Electrospinning technique

Recently, electrospinning technique towards industrial applications has drawn special research interests. It is a method of spinning polymer fibres making them into nanosized fibres with potentially excessive length [210], controllable porosity [211], 3D topography [212] and functional characteristics [213]. Several comprehensive reviews are available to understand more about electrospinning and their potential applications in the field of biomedicine, filtration and sorption processes [214–217]. Fig. 10 shows the schematic diagram of a typical electrospinning apparatus [218]. In a strong electric field, the very thin charged jets of spinning polymer solution are formed from the needle and collected by the anode surface. This technique permits the continuous production of single or multi-filament materials, and the electrospun products display different textural properties depending on the evaporation rate and miscibility of solvent, polymer, and other

Table 2 — Assessment of potential approaches to process powder materials[198—227].

Method	Scheme	Description	Production volume	Binder
Uniaxial pressing		Mix the active component with/without binder and press into moulds	Low	Application dependant
Coating		Deposit coating on chosen substrate	Medium	Application dependant
Foaming		Incorporate gas into particulate suspension and dry into foam	High	Yes
Templating		Use solid/emulsion templates to form desired shapes and ordered morphology	Low	No
Casting		Cast particulate slurry on different substrates	Medium	Yes

Granulation	Mix the active component with binder and granulate to form pellets	High	Yes
Extrusion	Mix the active component with binder, extrude and cut into different desired lengths	High	Yes
Pulsed current processing	Subject powder bodies to pulsed electrical current and compressive stress to form strong powder bodies	Medium	No

parameters employed. By adjusting these parameters, a porous or core–shell morphology can be fabricated [219].

For the processing of powder materials, electrospinning technique can be used to incorporate the fine particles into carbon nanofibers. Generally, the stabilization and carbonization processes follow the electrospinning step to stabilize the polymer and generate more porous structure. As shown in Fig. 11, the pathways between the metal catalyst and the pore structures can provide access for hydrogen molecules to penetrate deep into the fibres reaching the metal catalyst [220].

The studied composite materials so far for hydrogen storage are carbon nanofibers [221], metal/metal oxides carbon fibres [222], metal-carbon-fluorine system [223], carbon-coated Li_3N nanofibers [224], Co-electrospun Pd-coated porous carbon nanofibers [225], and $LaNi_5$ nanofibers [226]. Thanks to these earlier contributions, the electrospinning technique opens up a prospective route to process powder hydrogen storage materials. For instance, nanofiberous composites with 3D porosity can be generated by encapsulation of MOF crystals [227]. Therefore, electrospinning presents a promising option for the system integration of powder materials into hydrogen storage units.

Concept of storing hydrogen in para form

Hydrogen storage for practical applications has been investigated for several decades. However, an effective materials-based solution is yet to come close to the market. To date, the common practice stays as storing pressurized hydrogen in high-pressure rated cylinders. The concept therefore needs to be changed around to work out in this regard.

Ortho-hydrogen and para-hydrogen

The existence of two forms of molecular hydrogen i.e. ortho-hydrogen and para-hydrogen, has been known to physicists and chemists for almost 90 years [228]. As shown in Fig. 12 [229], ortho-hydrogen is in a higher energy state than para-hydrogen. At first scientists were just inquisitive about the nature of the ortho- and para-hydrogen. Thanks to the rapid development in cryogenic hydrogen technology which gave more relevance to the difference between the two forms [230–234]. The equilibrium mass fractions of ortho-para hydrogen are temperature dependent as described by Eq. (4) [235]:

$$X_p = \frac{X_o}{3} \cdot \frac{1 + 5 \cdot e^{-6 \cdot \frac{86.2}{T}}}{3 \cdot e^{-2 \cdot \frac{86.2}{T}} + 7 \cdot e^{-12 \cdot \frac{86.2}{T}}} \qquad (4)$$

where e is the equilibrium concentrations; X_p is the mass fraction of para-hydrogen and X_o is the mass fraction of ortho-hydrogen.

As listed in Table 3, hydrogen at room temperature (300 K) is a mixture of 75% ortho-hydrogen and 25% para-hydrogen, and below room temperature the composition of ortho-para fraction varies. When temperature decreases to 20 K (liquid hydrogen), 100% para-hydrogen can be achieved [236,237].
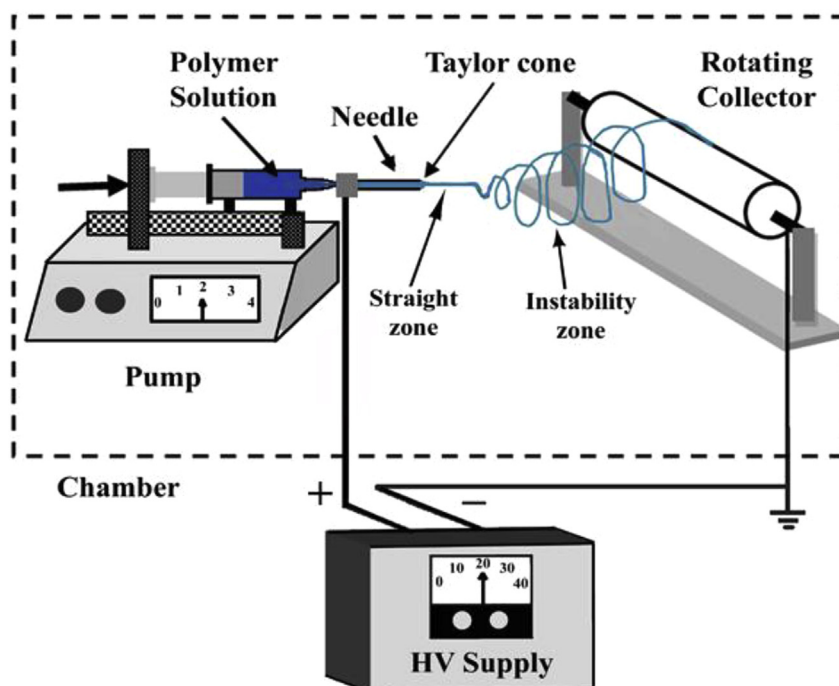
Fig. 10 — Schematic diagram of a general type of electrospinning apparatus. Re-produced from Ref. [124] with permission. Copyright 2007 the American Chemical Society.
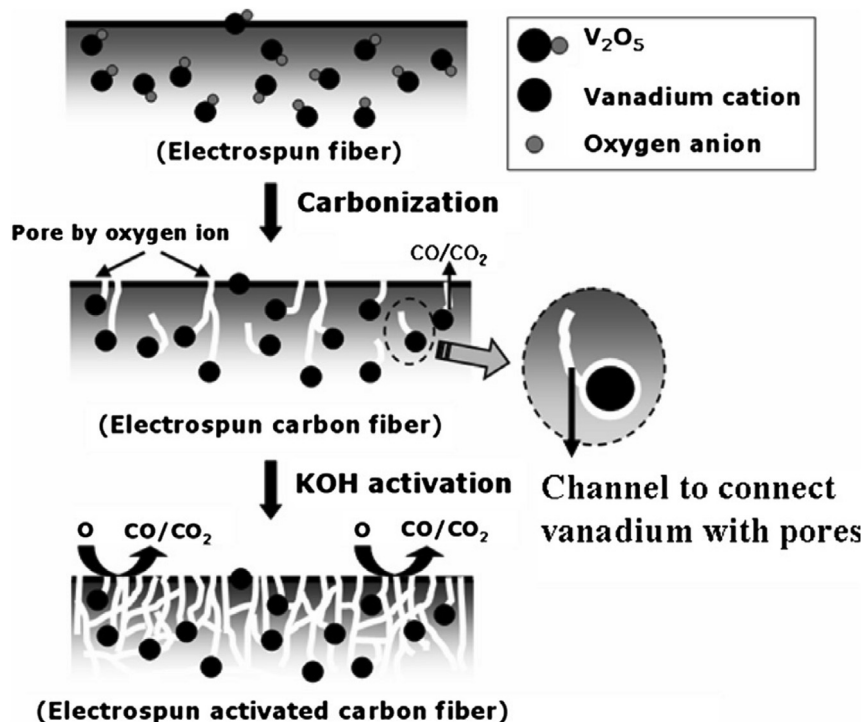
Fig. 11 — The schematic diagram of the formed pores by electrospinning process. Re-produced from Ref. [220] with permission. Copyright 2008 Elsevier.

Interests to hydrogen storage practices

The interest in the concept of storing hydrogen in para form stems from the fact that para-hydrogen has a lower energy state than ortho-hydrogen. It is therefore theoretically easier to store hydrogen in the para form. The equilibrium fraction of para-hydrogen is known to evolve to 100% as the temperature reaches 20 K. In an isolated state however, the conversion from ortho- to para-hydrogen follows slow kinetics and takes several days to complete, and thus the development of an
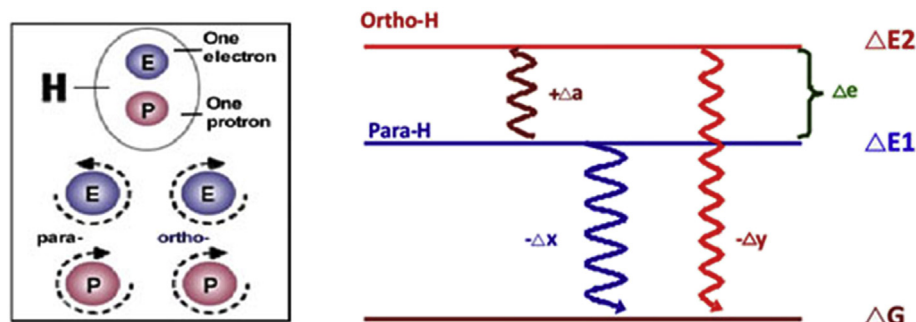
Fig. 12 – Ortho-hydrogen and para-hydrogen. Ortho-hydrogen is in the higher energy state then para-hydrogen. Reproduced from Ref. [228] with permission.

effective way to convert hydrogen from ortho form to para form becomes critical. Two primary approaches were provided to induce the ortho-para hydrogen transition [234]. In the first approach, hydrogen molecules are dissociated into atoms, which are then allowed to recombine. In the dissociated state, the two atomic nuclei are no more oriented with regards to nuclear spins. As the hydrogen atoms recombine, the generation of molecules depends on the equilibrium energy distribution dictated by the temperature. In the second approach, there is an influence of an inhomogeneous magnetic field on the nuclear magnetic field of the hydrogen molecule. The applied external field would trigger a spin reversal corresponding to an ortho-para transition. It is a necessity for the hydrogen molecule to be sufficiently close to the magnetic specie for the field to have an influence on the hydrogen molecule.

In practice, the transition mechanism is catalysed by any technique which is capable of producing hydrogen atoms or at least destroying the molecular bond between the two nuclei. Fukutani et al. [229a] reviewed the ortho-para conversion of molecular hydrogen on solid surfaces, and concluded that the conversion can be promoted in a physisorption state through interaction with surfaces of magnetic as well as diamagnetic

materials such as Cu, Ag, graphite, Si, ice and MOFs. Kosone et al. [238] reported that ortho-para transition can occur on non-magnetic solids and applying an electric field can induce the catalytic hydrogen ortho-para conversion. Some early work and calculations [86,239—242] also demonstrated that an applied field can considerably ease the binding of hydrogen molecules on specific hydrogen storage materials via dissociative adsorption and diffusion on the surface. In the presence of an electric field, the binding energy per hydrogen molecule would increase to promote sorption, and removal of the applied field leads to the absorbed hydrogen atoms being released efficiently. Therefore, the applied electric field can operate as a switch for hydrogen uptake/release processes Other studies [243—245] investigated the conversion of ortho-para hydrogen on several catalysts such as Cr_2O_3, Fe-modified zeolite and $LaFeO_3/Al_2O_3$ at 77 K. The results revealed that the spin conversion process was strongly dependent on a number of factors including BET surface area, morphology, calcination temperature and magnetic properties of the catalysts used. Another solution [246] was put forward involving the introduction of a dielectric coating onto porous activated carbon, in order to attain higher hydrogen storage capacity. Enhanced hydrogen storage was observed, which was attributed to the stronger interaction between charged carbon surface and polarized hydrogen molecules resulting from field induced polarization of TiO_2 coating. Considering the para-ortho conversion, a 2D axisymmetric geometric hydrogen storage model was developed for predicting the combined heat and mass transfer of the storage system [247]. It was reported that the conversion enables the filling of more hydrogen in the storage tank. Some measurement on a cryogenic adsorption hydrogen storage system indicated that the temperature-dependent conversion of ortho-para hydrogen was enhanced by the catalytic activity of the adsorption materials in the tank such as iron-benzene-1,3,5-tricarboxylate xerogel (Fe-BTC), and the energy balance must be taken into consideration in thermal analyses [248].

To enable long-term hydrogen storage, the transition from para-hydrogen to ortho-hydrogen must be prevented in the system. The interaction of para-hydrogen with a paramagnetic catalyst was reported to induce the conversion to ortho-hydrogen [249]. Oxygen contamination would also trigger the conversion of para-hydrogen to ortho-hydrogen [250]. Therefore, the minimization of oxygen contamination is required for a long-term storage of hydrogen. An

Temperature (K)	Equilibrium fraction of para hydrogen (%)	Heat of conversion from normal to para (kJ/kg)
20	99.821	527.138
30	97.012	527.138
40	88.727	527.117
50	77.054	526.845
60	65.569	525.531
70	55.991	521.770
78	50.028	515.500
80	48.537	513.932
90	42.882	500.757
100	38.620	481.671
120	32.959	427.248
150	28.603	322.495
200	25.974	163.774
250	25.264	70.524
300	25.072	27.562

Table 3 – Temperature-dependant equilibrium of ortho-para hydrogen [236].
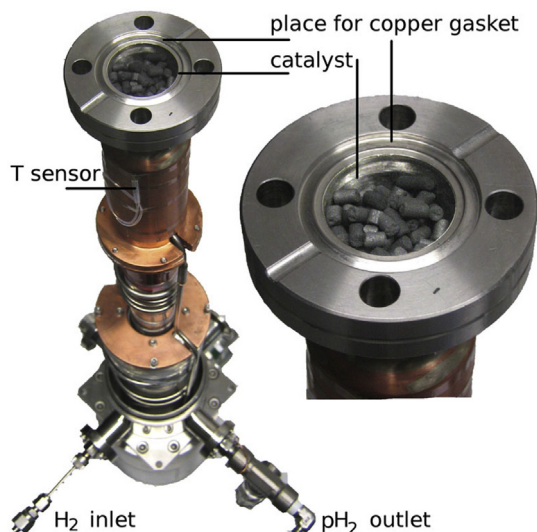
Fig. 13 – Photographs of a two-stage cryocooler with open catalyst chamber, filled with (rods of) activated charcoal, which was later replaced by iron(III) oxide (hydrate) of smaller mesh size (300–500 mm), which enabled higher production rates. Re-produced from Ref. [253] with permission. Copyright 2012 John Wiley & Sons, Ltd.

experimental study [251] revealed that para-ortho hydrogen conversion became active after 10–15 days of dormancy when hydrogen temperature reached 70–80 K. This conversion moved towards equilibrium in 25–30 days when the vessel's temperature reached 100–120 K at ~50 g·L^{-1} density. A dynamic model was developed to characterize dormancy and loss of hydrogen from an insulated cryogenic pressure vessel [252]. Under the conditions employed in the study, endothermic heat absorption was shown to extend the loss-free dormancy period by 85% if the tank was initially 75% full. However, if the tank was initially 100% full, the effect was not significant since the tank reached the maximum allowable

pressure prior to the conversion of a significant fraction of para-hydrogen to ortho-hydrogen.

Para-hydrogen converter

The production and storage of hydrogen in para form is crucial for long-term hydrogen storage solutions. Para-hydrogen can be produced through thermal equilibrium transitions, and near a temperature of 20 K the para-hydrogen fraction is nearly 100%. However, in the absence of catalysts, the rate of such inter-conversion is extremely slow. Enrichment of para-hydrogen can be performed by passing extra-pure hydrogen gas though a catalyst bed at low temperature. To prevent the re-establishment of the room temperature thermal equilibrium, it is better to store the enriched para-hydrogen in a cylinder with aluminium liner, since steel cylinders have paramagnetic properties that would catalyse the conversion rate of para-hydrogen to ortho-hydrogen. The ortho-para conversion is most efficient if done at the temperature of liquid nitrogen (77 K) in the presence of a catalyst.

Hövener et al. [253] developed a continuous-flow, high-throughput and high-pressure para-hydrogen converter, as shown in Fig. 13. It was a two-stage, closed-cycle helium cryocooler with open catalyst chamber, and the use of iron (III) oxide hydrate with a particle size of 300–500 μm was reported to be efficient [254]. Fig. 14 shows the schematic view of the para-hydrogen production unit. In order to adhere to safety requirements, the unit was divided into two parts. One part consisting of the electronic devices was kept inside a maintenance building in the attic of the institute. The other part consisting of all H$_2$-containing parts including the cold head and bulk H$_2$ bottles, were mounted on the outside, and the connections were done through a wall of about 30 cm, and sealed [253].

The unit generates a continuous flow of 4 L·min^{-1} of 98% enriched para-hydrogen at a maximum pressure of 50 bar. The time required for the complete production cycle, including cleaning and cooling to 25 K, is less than 5 h, and the actual conversion to para-hydrogen takes only 45 min of this time.
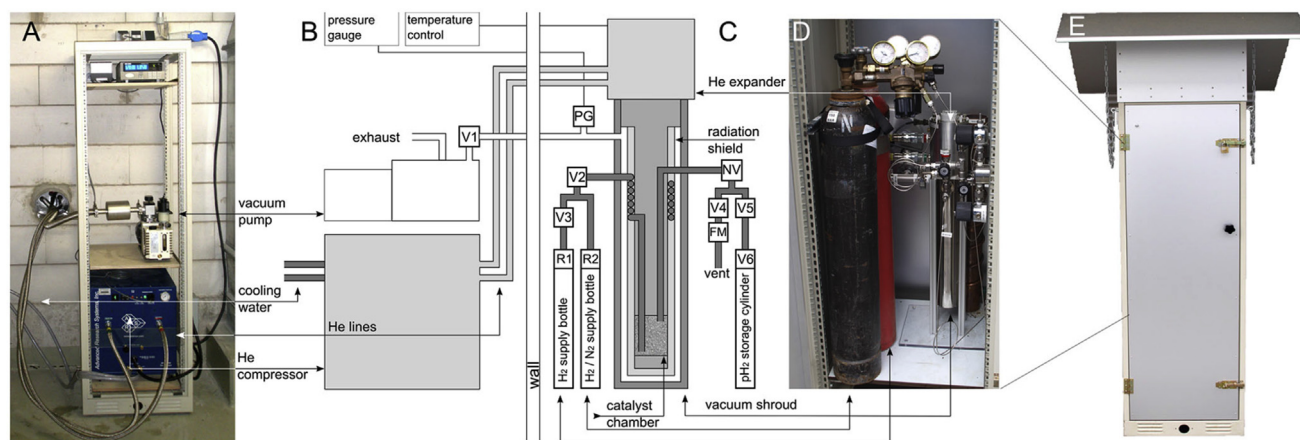
Fig. 14 – Photographs and schematic view of the para-hydrogen production unit: (A) helium compressor, vacuum pump, temperature and pressure control; (B, C) schematic representation; (D) H$_2$, N$_2$ supply bottles, cold head; (E) external housing. To comply with safety, the electronics (A, B) and H$_2$-containing parts (C–E) were separately installed on the inside and outside of a maintenance building on the roof of the institute, respectively. FM, flowmeter; (N) V, (needle) valve; PG, pressure gauge; R, pressure regulator. Re-produced from Ref. [253] with permission. Copyright 2012 John Wiley & Sons, Ltd.

Conclusions

In the last decade, significant progress has been made in the search for suitable materials and concepts for hydrogen storage, yet no hydrogen storage systems have been developed that satisfy all the 2020 DOE targets. It is therefore essential to develop durable low-cost hydrogen storage systems with high usable storage capacity and suitable kinetic and thermodynamic characteristics.

Four key conclusions can be drawn from this critical review on the state-of-the-art in materials-based hydrogen storage solutions. Firstly, for porous materials, many efforts have been devoted towards the development of new materials with higher surface area and larger free volume. As reviewed from the literature, only less than 1 wt.% hydrogen adsorption capacities for porous materials were experimentally reported at ambient conditions, even for materials selected with higher BET surface areas. Furthermore, at 77 K and ambient pressure, the enhancement of hydrogen storage capacities caused by increased surface area larger than 2000 $m^2 \cdot g^{-1}$ is quite limited. Therefore, attention should be focused on increasing reaction enthalpies up to ~20 $kJ \cdot mol^{-1}$, and it can theoretically be accomplished by introduction of Kubas binding, ionization, polarization and irradiation of the host materials as well as inducing H_2 spillover effect. However, there is no substantial progress on Kubas binding and H_2 spillover effect for H_2 storage applications in the last 10 years.

Secondly, for metal/chemical hydrides, the key aspect is to enhance the thermodynamics and kinetics of hydrogen release and uptake. In terms of kinetics, nanoconfinement of the hydride materials can be an effective way to reduce their particle sizes and tailor the kinetics of hydrogen charge and discharge. With regards to thermodynamics, selection of less stable hydrides is a meaningful direction. Another promising approach is to develop more advanced ionic liquids as liquid hydrogen storage materials, or use ionic liquids as catalytic/supporting solvents to achieve synergistic effect in the chemical hydrides systems.

Thirdly, the processing techniques of solid-state materials towards system integration such as shaping and electrospinning processes will be necessary to facilitate the transition of developed materials from lab to applications. We are mindful that other techniques may crop up with applicability in the processing of solid-state hydrogen storage materials towards system integration.

Fourthly, the concept of storing hydrogen in the para form was put forward due to the lower energy state of para-hydrogen. To enable long-term hydrogen storage at ambient condition, a converter of ortho-to-para hydrogen was demonstrated for the proof-of-concept. Thanks to these earlier contributions, significant advances in hydrogen storage continue to be made; we are still keen to see new concepts or developments emerging with regards to hydrogen storage solutions.

Acknowledgements

REFERENCES

[1] http://peakoilbarrel.com/world-energy-2014-2050-part-3. [Accessed 11 October 2015].

[2] Shafiee S, Topal E. When will fossil fuel reserves be diminished? Energy Policy 2009;37:181–9.

[3] Balat M, Balat H. Resent trends in global production and utilization of bio-ethanol fuel. Appl Energy 2009;86:2273–82.

[4] Dresselhaus MS, Thomas IL. Alternative energy technologies. Nature 2001;414:332–7.

[5] Dunn S. Hydrogen futures: toward a sustainable energy system. Int J Hydrogen Energy 2002;27:235–64.

[6] Tour JM, Kittrell C, Colvin VL. Green carbon as a bridge to renewable energy. Nat Mater 2010;9:871–4.

[7] Von Helmolt R, Eberle U. Fuel cell vehicles: status 2007. J Power Sour 2007;165:833–43.

[8] (a)http://energy.gov/eere/fuelcells/doe-technical-targets-onboard-hydrogen-storage-light-duty-vehicles.(b)http://energy.gov/eere/fuelcells/doe-technical-targets- onboard-hydrogen -storage-light-duty-vehicles. [Accessed 22 October 2015].

[9] Stetson N. An overview of U.S. DOE's activities for hydrogen fuel cell technologies, 2/27/2012, Clearwater, Floride, America.

[10] Stroman RO, Schuette MW, Swider-Lyons K, Rodgers JA, Edwards DJ. Liquid hydrogen fuel system design and demonstration in a small long endurance air vehicle. Int J Hydrogen Energy 2014;39:11279–90.

[11] Van den berg AWC, Areán CO. Materials for hydrogen storage: current research trends and perspectives. Chem Commun 2008:668–81.

[12] McWhorter S, Read C, Ordaz G, Stetson N. Materials-based hydrogen storage: attributes for near-term, early market PEM fuel cells. Curr Opin Solid State Mater 2011;15:29–38.

[13] Sakintuna B, Lamari-Darkrim F, Hirscher M. Metal hydride materials for solid hydrogen storage: a review. Int J Hydrogen Energy 2007;32:1121–40.

[14] Martínew-Mesa A, Serfert G. Adsorption of molecular hydrogen on nanostructured surfaces. Rev Cub Fis 2014;31:32–4.

[15] Broom DP, Webb CJ, Hurst KE, Parilla PA, Gennett T, Brown CM, et al. Outlook and challenges for hydrogen storage in nanoporous materials. Appl Phys A 2016;122:151.

[16] Oelerich W, Klassen T, Bormann R. Metal oxides as catalysts for improved hydrogen sorption in nanocrystalline Mg-based materials. J Alloy Compd 2001;315:237–42.

[17] Zhou L. Progress and problems in hydrogen storage methods. Renew Sustain Energy Rev 2005;9:395–408.

[18] Gross KJ, Thomas GJ, Jensen CM. Catalyzed alanates for hydrogen storage. J Alloy Compd 2002;330–332:683–90.

[19] Eigen N, Kunowsky M, Klassen T, Bormann R. Synthesis of NaAlH$_4$-based hydrogen storage material using milling under low pressure hydrogen atmosphere. J Alloy Compd 2007;430:350–5.

[20] Orimo SI, Nakamori Y, Eliseo JR, Züttel A, Jensen CM. Complex hydrides for hydrogen storage. Chem Rev 2007;107:4111–32.

[21] Wilkes JS. A short history of ionic liquids-from molten salts to neoteric solvent. Green Chem 2002;4:73–80.

[22] Hajipour AR, Rafiee F. Recent progress in ionic liquids and their applications in organic synthesis. Org Prep Proced Int 2015;47:249−308.

[23] Dupont J. On the solid, liquid and solution structural organization of imidazolium ionic liquids. J Braz Chem Soc 2004;15:341−50.

[24] Hallett JP, Welton T. Room-temperature ionic liquids: solvents for synthesis and catalysis. 2. Chem Rev 2011;111:3508−76.

[25] Ghandi K. A review of ionic liquids, their limits and applications. Green Sust Chem 2014;4:44−53.

[26] MacFarlane DR, Forsyth M, Howlett PC, Kar M, Passerini S, Pringle JM, et al. Ionic liquids and their solid-state analogues as materials for energy generation and storage. Nat Rev 2016;1:1−14.

[27] Barghi SH, Tsotsis TT, Sahimi M. Solubility and diffusivity of H_2 and CO_2 in the liquid [bmim][PF_6]. Int J Hydrogen Energy 2015;40:8713−20.

[28] Ahluwalia RK, Peng JK, Hua TQ. Hydrogen release from ammonia borane dissolved in an ionic liquid. Int J Hydrogen Energy 2011;36:15689−97.

[29] Stracke MP, Ebeling G, Cataluña R, Dupont J. Hydrogen-storage materials based on imidazolium ionic liquids. Energy Fuels 2007;21:1695−8.

[30] Sahler S, Sturm S, Kessler MT, Prechtl MHG. The role of ionic liquids in hydrogen storage. Chem Eur J 2014;20:8934−41.

[31] Su DS, Centi G. A perspective on carbon materials for future energy applications. J Energy Chem 2013;22:151−73.

[32] Yang JS, Jung H, Kim T, Park CR. Recent advances in hydrogen storage technologies based on nanoporous carbon materials. Prog Nat Sci 2012;22:631−8.

[33] Xia Y, Yang Z, Zhu Y. Porous carbon-based materials for hydrogen storage: advancement and challenges. J Mater Chem A 2013;1:9365−81.

[34] Rallapalli PBS, Raj MC, Patil DV, Prasanth KP, Somani RS, Bajaj HC. Activated carbon @MIL-101(Cr): a potential metal-organic framework composite material for hydrogen storage. Int J Energy Res 2013;37:746−53.

[35] Prabhakaran PK, Deschamps J. Doping activated carbon incorporated composite MIL-101 using lithium: impact on hydrogen uptake. J Mater Chem A 2015;3:7014−21.

[36] Lim KL, Kazemian H, Yaakob Z, Daud WRW. Solid-state materials and methods for hydrogen storage: a critical review. Chem Eng Tech 2010;33:213−26.

[37] Getman RB, Bae YS, Wilmer CE, Snurr RQ. Review and analysis of molecular simulations of methane, hydrogen, and acetylene storage in metal-organic frameworks. Chem Rev 2012;112:703−23.

[38] Durbin DJ, Malardier-Jugroot. Review of hydrogen storage techniques for on board vehicle applications. Int J Hydrogen Energy 2013;38:14595−617.

[39] Langmi HW, Ren JW, North B, Mathe M, Bessarabov D. Hydrogen storage in metal-organic frameworks. A review. Electrochim Acta 2014;128:368−92.

[40] Jena P. Materials for hydrogen storage: past, present, and future. J Phys Chem Lett 2011;2:206−11.

[41] Tozzini V, Pellegrini V. Prospects for hydrogen storage in graphene. Phys Chem Chem Phys 2013;15:80−9.

[42] Kabbour H, Baumann TF, Satcher JH, Saulnier A, Ahn CC. Toward new candidates for hydrogen storage: high-surface-area carbon aerogels. Chem Mater 2006;18:6085−7.

[43] Furukawa H, Ko N, Go YB, Aratani N, Choi SB, Choi E, et al. Ultrahigh porosity in metal-organic frameworks. Science 2010;329:424−8.

[44] Farha OK, Eryazici I, Jeong NC, Hauser BG, Wilmer CE, Sarjeant AA, et al. Metal-organic framework materials with ultrahigh surface areas: is the sky the limit? J Am Chem Soc 2012;34:15016−21.

[45] Suh MP, Park HJ, Prasad TK, Lim DW. Hydrogen storage in metal-organic frameworks. Chem Rev 2012;112:782−835.

[46] Frost H, Düren T, Snurr RQ. Effects of surface area, free volume, and heat of adsorption on hydrogen uptake in metal-organic frameworks. J Phys Chem B 2006;110:9565−70.

[47] Wu H, Chua YS, Krungleviciute V, Tyagi M, Chen P, Yildirim Y, et al. Unusual and highly tunable missing-linker defects in zirconium metal-organic framework UiO-66 and their import effects on gas adsorption. J Am Chem Soc 2013;135:10525−32.

[48] Kozachuk O, Luz I, Llabrés I, Xamena FX, Noei H, Kauer M, et al. Multifunctional, defect-engineered metal-organic frameworks with ruthenium centers: sorption and catalytic properties. Angew Chem Int Ed 2014;53:7058−62.

[49] Felderhoff M, Weidenthaler C, von Helmolt R, Eberle U. Hydrogen storage: the remaining scientific and technological challenges. Phys Chem Chem Phys 2007;9:2643−53.

[50] Reardon H, Hanlon JM, Hughes RW, Godula-Jopek A, Mandal TK, Gregory DH. Emerging concepts in solid-state hydrogen storage: the role of nanomaterials design. Energy Environ Sci 2012;5:5951−79.

[51] Bhatia SK, Myers AL. Optimum conditions for hydrogen storage. Langmuir 2006;22:1688−700.

[52] Zhao Y, Kim Y, Dillon AC, Heben MJ, Zhang SB. Hydrogen storage in novel organometallic buckyballs. Phys Rev Lett 2005;94:155504.

[53] Hamaed A, Hoang TKA, Trudeau M, Antonelli DM. Optimization of hydrogen storage capacity in silica-supported low valent Ti systems exploiting Kubas binding of hydrogen. J Organomet Chem 2009;694:2793−800.

[54] Züttle A. Materials for hydrogen storage. Mater Today 2003;6:24−33.

[55] Fichtner M. Nanotechnological aspects in materials for hydrogen storage. Adv Eng Mater 2005;7:443−55.

[56] Bhatia SK, Myers AL. Optimum conditions for adsorptive storage. Langmuir 2006;22:1688−700.

[57] Dillon AC, Parilla PA, Zhao Y, Kim YH, Gennett T, Curtis C, Blackburn JL, Gilbert KEH, Alleman JL, Jones KM, Zhang SB, Heben MJ. NREL activities in DOE Carbon-based Materials Center of Excellence. www.hydrogen.energy.gov/pdfs/review05/stp_63_heben.pdf. [Accessed 18 October 2014].

[58] Züttle A, Sudan P, Mauron P, Kiyobayashi T, Emmenegger C, Schlapbach L. Hydrogen storage in carbon nanostructures. Int J Hydrogen Energy 2002;27:203−12.

[59] Hu X, Skadtchenko BO, Trudeau M, Antonelli DM. Hydrogen storage in chemically reducible mesoporous and microporous Ti oxides. J Am Chem Soc 2006;128:11740−1.

[60] Zhou W, Wu H, Hartman HR, Yildirim T. Hydrogen and methane adsorption in metal-organic frameworks: a high-pressure volumetric study. J Phys Chem C 2007;111:16131−7.

[61] Kubas GJ, Ryan RR, Swanson BI, Vergamini PJ, Wasserman HJ. Characterization of the first examples of isolable molecular hydrogen complexes, $M(CO)_3(PR_3)_2(H_2)$ (M=Mo, W; R=Cy, i-Pr). Evidence for a side-on bonded H_2 ligand. J Am Chem Soc 1984;106:451−2.

[62] Kubas GJ. Molecular hydrogen complexes: coordination of a σ bond to transition metals. Acc Chem Res 1988;21:120−8.

[63] Kubas GJ. Metal-dihydrogen and sigma-bond coordination: the consummate extension of the Dewar-Chatt-Duncanson model-olefin π bonding. J Organometal Chem 2001;635:37−68.

[64] Kubas GJ. Fundamentals of H_2 binding and reactivity on transition metals underlying hydrogenase function and H_2 production and storage. Chem Rev 2007;107:4152−205.

[65] Hoang TKA, Antonelli DM. Exploiting the Kubas interaction in the design of hydrogen storage materials. Adv Mater 2009;21:1787–800.

[66] Hoang TKA, Webb MI, Mai HV, Hamaed A, Walsby CJ, Trudeau M, et al. Design and synthesis of vanadium hydrazide gels for Kubas-type hydrogen adsorption: a new class of hydrogen storage materials. J Am Chem Soc 2010;132:11792–8.

[67] Skipper CVJ, Hamaed A, Antonelli DM, Kaltsoyannis N. Computational study of silica-supported transition metal fragments for Kubas-type hydrogen storage. J Am Chem Soc 2010;132:17296–305.

[68] Skipper CVJ, Hoang TKA, Antonelli DM, Kaltsoyannis N. Transition metal hydrazide-based hydrogen-storage materials: the first atoms-in-molecules analysis of the Kubas interaction. Chem Eur J 2012;18:1750–60.

[69] Mai HV, Hoang TKA, Hamaed A, Trudeau M, Antonelli DM. Cyclopentadienyl chromium hydrazide gels for Kubas-type hydrogen storage. Chem Commun 2010;46:3206–8.

[70] Hamaed A, Hoang TKA, Moula G, Aroca R, Trudeau ML, Antonelli DM. Hydride-induced amplification of performance and binding enthalpies in chromium hydrazide gels for Kubas-type hydrogen storage. J Am Soc Chem 2011;133:15434–43.

[71] Lochan RC, Head-Gordon M. Computational studies of molecular hydrogen binding affinities: the role of dispersion forces, electrostatics, and orbital interactions. Phys Chem Chem Phys 2006;8:1357–70.

[72] Shin WH, Yang SH, Goddard WA, Kang JK. Ni-dispersed fullerenes: hydrogen storage and desorption properties. Appl Phys Lett 2006;88:053111.

[73] Lee JW, Kim HS, Lee JY, Kang JK. Hydrogen storage and desorption properties of Ni-dispersed carbon nanotubes. Appl Phys Lett 2006;88:143126.

[74] Shevlin SA, Guo ZX. Transition-metal-doping-enhanced hydrogen storage in boron nitride systems. Appl Phys Lett 2006;89:153104.

[75] Durgun E, Ciraci S, Zhou W, Yildirim T. Transition-metal-ethylene complexes as high-capacity hydrogen-storage media. Phys Rev Lett 2006;97:226102.

[76] Lee H, Choi WI, Ihm J. Combinatorial search for optimal hydrogen-storage nanomaterials based on polymers. Phys Rev Lett 2006;97:056104.

[77] Mingos DMP. A historical perspective on Dewar's Landmark contribution to organometallic chemistry. J Organomet Chem 2001;635:1–8.

[78] Srinivasu K, Chandrakumar KRS, Ghosh SK. Computational investigation of hydrogen adsorption by alkali-metal-doped organic molecules: role of aromaticity. Chem Phys Chem 2009;10:427–35.

[79] Niu J, Rao BK, Jena P, Manninen M. Interaction of H_2 and He with metal atoms, clusters and ions. Phys Rev B 1995;51:4475–84.

[80] Stefanakos L. Fuel cell and hydrogen research. The 2005 annual DOE hydrogen program merit review presentation (STP 48). May 23–25, 2005. Washington, DC.

[81] Liu CS, Zeng Z. Ionization-induced enhancement of hydrogen storage in metalized C_2H_4 and C_5H_5 molecules. Phys Rev B 2009;79:245419.

[82] Guo JH, Zhang H, Miramoto Y, Cheng XL. The effect of ionization and CH_3 ligand for hydrogen storage in Co- and Ni-based organometallic compounds. Int J Quantum Chem 2011;111:4443–51.

[83] Wang K, Liu ZF, Wang XQ, Cui XD. Enhancement of hydrogen binding affinity with low ionization energy Li2F coating on C60 to improve hydrogen storage capacity. Int J Hydrogen Energy 2014;39:15639–45.

[84] Yaghi OM, Matzder AJ. New concepts for optimized hydrogen storage in MOFs. The 2005 annual DOE hydrogen program merit review presentation (STP52). May 23–25, 2005. Washington, DC.

[85] Yoon M, Yang SY, Wang E, Zhang ZY. Charged fullerenes as high-capacity hydrogen storage media. Nano Lett 2007;7:2578–83.

[86] Zhou J, Wang Q, Sun Q, Jena P, Chen XS. Electric field enhanced hydrogen storage on polarisable materials substrates. PNAS 2010;107:2801–6.

[87] Yoon M, Yang S, Hicke C, Wang E, Geohegan D, Zhang Z. Calcium as the superior coating metal in functionalization of carbon fullerenes for high-capacity hydrogen storage. Phys Rev Lett 2008;100:206806–9.

[88] Muga LG, Muga B. Hydrogen adsorption on irradiated carbon and other materials. The 2005 annual DOE hydrogen program merit review presentation (STP54). May 23–25, 2005. Washington, DC.

[89] Alivisatos AP, Cohen ML, Frechet JMJ, Head-Gordon M, Long JR, Louie SG, et al. A synergistic approach to the development of new hydrogen storage materials. The 2005 annual DOE hydrogen program merit review presentation (ST 8). May 23–25, 2005. Washington, DC.

[90] Obolensky MA, Basteev AV, Bazyma LA. Hydrogen storage in irradiated low-dimensional structures. Fuller Nanotub Carbon Nanostruct 2011;19:133–6.

[91] Novaković JG, Lj Matović, Drvendžija M, Novaković N, Rajnović D, Šiljegović M, et al. Changes of hydrogen storage properties of MgH_2 induced by heavy ion irradiation. Int J Hydrogen Energy 2008;33:1876–9.

[92] Wang LF, Yang RT. Hydrogen storage on carbon-based adsorbents and storage at ambient temperature by hydrogen spillover. Catal Rev 2010;52:411–61.

[93] Boudart M, Vannice MA, Benson JE. Adlineation, portholes and spillover. Phys Chem Neue Folge 1969;64:171–7.

[94] Juárez JM, Gómez Costa MB, Anunziata OA. Synthesis and characterization of Pt-CMK-3 hybrid nanocomposite for hydrogen storage. Int J Energy Res 2015;39:128–39.

[95] Wang LF, Yang RT. New sorbents for hydrogen storage by hydrogen spillover. Energy Environ Sci 2008;1:268–79.

[96] Prins R. Hydrogen spillover. Facts and fiction. Chem Rev 2012;112:2714–38.

[97] Psofogiannakis GM, Froudakis GE. Fundamental studies and perceptions on the spillover mechanism for hydrogen storage. Chem Commun 2011;47:7933–43.

[98] Chen H, Wang LF, Yang J, Yang RT. Investigation on hydrogenation of metal-organic frameworks HKUST-1, MIL-53, and ZIF-8 by hydrogen spillover. J Phys Chem C 2013;117:7565–76.

[99] Wang CY, Tsao CS, Yu MS, Liao PY, Chung TY, Wu HC, et al. Hydrogen storage measurement, synthesis and characterization of metal-organic frameworks via bridged spillover. J Alloy Compd 2010;492:88–94.

[100] Yang SJ, Cho JH, Nahm KS, Park CR. Enhanced hydrogen storage capacity of Pt-loaded CNT@MOF-5 hybrid composites. Int J Hydrogen Energy 2010;35:13062–7.

[101] Li YW, Yang RT. Significantly enhanced hydrogen storage in metal-organic frameworks via spillover. J Am Chem Soc 2006;128:726–7.

[102] Li QX, Lueking AD. Effect of surface oxygen groups and water on hydrogen spillover in Pt-doped activated carbon. J Phys Chem C 2011;115:4273–82.

[103] Lin KS, Adhikari AK, Chang KC, Tu MT, Lu W. Hydrogen adsorption in metal-organic frameworks by hydrogen spillover. Catal Today 2011;164:23–7.

[104] Anbia M, Mandegarzad S. Enhanced hydrogen sorption on modified MIL-101 with Pt/CMK-3 by hydrogen spillover effect. J Alloy Compd 2012;532:61–7.

[105] Li BY, Huang X, Gong RN, Ma MR, Yang XJ, Liang LY, et al. Catalyzed hydrogen spillover for hydrogen storage on

microporous organic polymers. Int J Hydrogen Energy 2012;37:12813—20.

[106] Wang LF, Stuckert NR, Chen H, Yang RT. Effects of Pt particle size on hydrogen storage on Pt-doped metal-organic framework IRMOF-8. J Phys Chem C 2011;115:4793—9.

[107] Lueking AD, Yang RT. Hydrogen spillover to enhance hydrogen storage-study of the effect of carbon physicochemical properties. Appl Catal A 2004;265:259—68.

[108] Li Y, Yang RT. Hydrogen storage in metal-organic frameworks by bridged hydrogen spillover. J Am Chem Soc 2006;128:8136—7.

[109] Stuckert NR, Wang LF, Yang RT. Characteristics of hydrogen storage by spillover on Pt-deped carbon and catalyst-bridged metal-organic framework. Langmuir 2010;26:11963—71.

[110] Lachawiec Jr AJ, Qi G, Yang RT. Hydrogen storage in nanostructured carbons by spillover: bridge-building enhancement. Langmuir 2005;21:11418—24.

[111] Ardelean O, Blanita G, Borodi G, Mihet M, Coros M, Lupu D. On the enhancement of hydrogen uptake by IRMOF-8 composites with Pt/carbon catalyst. Int J Hydrogen Energy 2012;37:7378—84.

[112] Li YW, Yang RT, Liu CJ, Wang Z. Hydrogen storage on carbon doped with platinum nanoparticles using plasma reduction. Ind Eng Chem Res 2007;46:8277—81.

[113] Psofogiannakis GM, Froudakis GE. Theoretical explanation of hydrogen spillover in metal-organic frameworks. J Phys Chem C 2011;115:4047—9.

[114] Ganz E, Dornfeld M. Energetics and thermodynamics of the initial stages of hydrogen storage by spillover on prototypical metal-organic framework and covalent-organic framework materials. J Phys Chem C 2014;118:5657—63.

[115] Guo JH, Zhang H, Tang YJ, Cheng XL. Hydrogen spillover mechanism on covalent organic frameworks as investigated by *ab initio* density functional calculation. Phys Chem Chem Phys 2013;15:2873—81.

[116] Cao WX, Li YW, Wang LM, Liao SJ. Effects of metal ions and ligand functionalization on hydrogen storage in metal-organic frameworks by spillover. J Phys Chem C 2011;115:13829—36.

[117] Campesi R, Cuevas F, Latroche M, Hirscher M. Hydrogen spillover measurements of unbridged and bridged metal-organic frameworks-revisited. Phys Chem Chem Phys 2010;12:10457—9.

[118] Luzan SM, Talyzin AV. Comment to the "Response to hydrogen adsorption in Pt catalyst/MOF-5 material" by Li et al. Micro Meso Mater 2011;139:216—8.

[119] Demirocak DE, Srinivasan SS, Ram MK, Goswami DY, Stefanakos EK. Volumetric hydrogen sorption measurements-uncertainty error analysis and the importance of thermal equilibration time. Int J Hydrogen Energy 2013;38:1469—77.

[120] Luzan SM, Talyzin AV. Hydrogen adsorption in Pt catalyst/MOF-5 materials. Micro Meso Mater 2010;135:201—5.

[121] Boukhvalov DW, Katsnelson MI, Lichtenstein AI. Hydrogen on grapheme: electronic structure, total energy, structural distortions and magnetism from first-principles calculations. Phys Rev B 2008;77:035427.

[122] Klyamkin SN, Chuvikov SV, Maletskaya NV, Kogan EV, Fedin VP, Kovalenko KA, et al. High-pressure hydrogen storage on modified MIL-101 metal-organic framework. Int J Energy Res 2014;38:1562—70.

[123] Zhu JL, Cheng JH, Dailly A, Cai M, Beckner M, Shen PK. One-pot synthesis of Pd nanoparticles on ultrahigh surface area 3D porous carbon as hydrogen storage materials. Int J Hydrogen Energy 2014;39:14843—50.

[124] Lucci FR, Darby MT, Mattera MFG, Ivimey CJ, Therrien AJ, Michaelides A, et al. Controlling hydrogen activation, spillover, and desorption with Pd-Au single-atom alloys. J Phys Chem Lett 2016;7:480—5.

[125] Nababo D, Niemantsverdriet JW, Chleys M, Van Steen E. Hydrogen spillover in the Fischer-Tropsch synthesis: an analysis of platinum as a promoter for cobalt-alumina catalysts. Catal Today 2016;261:17—27.

[126] Ruse E, Pevzner S, Bar IP, Nadiv R, Skripnyuk VM, Rabkin E, et al. Hydrogen storage and spillover kinetics in carbon nanotube-Mg composites. Int J Hydrogen Energy 2016;41:2814—9.

[127] Ensafi AA, Jafari-Asi M, Nabiyan A, Rezaei B, Dinari M. Hydrogen storage in hybrid of layered double hydroxides/reduced graphene oxide using spillover mechanism. Energy 2016;99:103—14.

[128] Kumar EM, Prajapat B, Saha B, Thapa R. Spillover of hydrogen on SiC-ML surface: doping effect and bond exchange mechanism. Int J Hydrogen Energy 2016;41:3928—39.

[129] Chung TY, Tsao CS, Tseng HP, Chen CH, Yu MS. Effects of oxygen functional groups on the enhancement of the hydrogen spillover of Pd-doped activated carbon. J Colloid Interface Sci 2015;441:98—105.

[130] Razzhivina IA, Badun GA, Chernysheva MG, Garshev AV, Shevchenko VP, Shevchenko K, et al. Hydrogen spillover through a gas phase. Mendeleev Commun 2016;26:59—60.

[131] Wu H. Strategies for the improvement of the hydrogen storage properties of metal hydride materials. ChemPhysChem 2008;9:2157—62.

[132] Eberle U, Felderhoff M, Schüth F. Chemical and physical solutions for hydrogen storage. Angew Chem Int Ed 2009;48:6608—30.

[133] Grzetz J. New approaches to hydrogen storage. Chem Sov Rev 2009;38:73—82.

[134] Pukazhselvan D, Kumar V, Singh SK. High capacity hydrogen storage: basic aspects, new developments and milestones. Nano Energy 2012;1:566—89.

[135] Vajo JJ, Skeith SL. Reversible storage of hydrogen in destabilized $LiBH_4$. J Phys Chem B 2005;109:3719—22.

[136] He T, Wu H, Wu GT, Wang JH, Zhou W, Xiong ZT, et al. Borohydride hydrazinates: high hydrogen content materials for hydrogen storage. Energy Environ Sci 2012;5:5686—9.

[137] Luo JH, Wu H, Zhou W, Kang XD, Fang ZZ, Wang P. $LiBH_4 \cdot NH_3BH_3$: a new lithium borohydride ammonia borane compound with a novel structure and favourable hydrogen storage properties. Int J Hydrogen Energy 2012;37:10750—7.

[138] Shin K, Kim Y, Strobel TA, Prasad PSR, Sugahara T, Lee H, et al. Tetra-n-butylammonium Borohydride semiclathrate: a hybrid material for hydrogen storage. J Phys Chem A 2009;113:6415—8.

[139] Ley MB, Jepsen LH, Lee YS, Cho YW, Bellosta von Colbe JM, Dornheim M, et al. Complex hydrides for hydrogen storage-new perspectives. Mater Today 2014;17:122—8.

[140] Bérubé V, Chen G, Dresselhaus MS. Impact of nanostructuring on the enthalpy of formation of metal hydrides. Int J Hydrogen Energy 2008;33:4122—31.

[141] Fichtner M. Properties of nanoscale metal hydrides. Nanotechnology 2009;20:204009.

[142] Zlotea C, Latroche M. Role of nanoconfinement on hydrogen sorption properties of metal nanoparticles hybrids. Colloids Surf A 2013;439:117—30.

[143] Wagemans RWP, van Lenthe JH, de Jongh PE, van Dillen AJ, de Jong KP. Hydrogen storage in magnesium clusters: quantum chemical study. J Am Chem Soc 2005;127:16675—80.

[144] Vajeeston P, Ravindran P, Fjellvag H. Theoretical investigations on low energy surfaces and nanowires of MgH$_2$. Nanotechnology 2008;19:275704.

[145] Vajeeston P, Ravindran P, Fjellvag H. Nanostructures of LiBH$_4$: a density-functional study. Nanotechnology 2009;20:275704.

[146] Kim KC, Dai B, Johnson JK, Sholl DS. Assessing nanoparticles size effects on metal hydride thermodynamics using the Wulff construction. Nanotechnology 2009;20:204001.

[147] Li ZY, Zhu GS, Lu GQ, Qiu SL, Yao XD. Ammonia borane confined by a metal-organic framework for chemical hydrogen storage: enhancing kinetics and eliminating ammonia. J Am Chem Soc 2010;132:1490–1.

[148] Gadipelli S, Ford J, Zhou W, Wu H, Udovic TJ, Yildirim T. Nanoconfinement and catalytic dehydrogenation of ammonia borane by magnesium-metal-organic-framework-74. Chem Eur J 2011;17:6043–7.

[149] Srinivas G, Ford J, Zhou W, Yildirim T. Zn-MOF assisted dehydrogenation of ammonia borane: enhanced kinetics and clean hydrogen generation. Int J Hydrogen Energy 2012;37:3633–8.

[150] Si XL, Sun LX, Xu F, Jiao CL, Li F, Liu SS, et al. Improved hydrogen desorption properties of ammonia borane by Ni-modified metal-organic frameworks. Int J Hydrogen Energy 2011;36:6698–704.

[151] Aijaz A, Karkamkar A, Choi XJ, Tsumori N, Rönnebro E, Autrey T, et al. Immobilizing highly catalytically active Pt nanoparticles inside the pores of metal-organic framework: a double solvents approach. J Am Chem Soc 2012;134:13926–9.

[152] Utke R, Thiangviriya S, Javadian P, Jensen TR, Milanese C, Klassen T, et al. 2LiBH$_4$-MgH$_2$ nanofined into carbon aerogel scaffold impregnated with ZrCl$_4$ for reversible hydrogen storage. Mater Chem Phys 2016;169:136–41.

[153] Thiangviriya S, Utke R. LiBH$_4$ nanoconfined in activated carbon nanofiber for reversible hydrogen storage. Int J Hydrogen Energy 2015;40:4167–74.

[154] Ngene P, Verkuijlen MHW, Barre C, Kentgens APM, De Jongh PE. Reversible Li-insertion on nanoscaffolds: a promising strategy to alter the hydrogen sorption properties of Li-based complex hydrides. Nano Energy 2016;22:169–78.

[155] Plerdsranoy P, Utke R. Ternary LiBH$_4$-MgH$_2$-NaAlH$_4$ hydride confined into nanoporous carbon host for reversible hydrogen storage. J Phys Chem Solids 2016;90:80–6.

[156] Callini E, Szilágyi PÁ, Paskevicius M, Stadie NP, Réhault J, Buckley CE, et al. Stabilization of volatile Ti(BH$_4$)$_3$ by nano-confinement I na metal-organic framework. Chem Sci 2016;7:666–72.

[157] Javadian P, Sheppard DA, Buckley CE, Jensen TR. Hydrogen storage properties of nanoconfined LiBH$_4$-Ca(BH$_4$)$_2$. Int J Hydrogen Energy 2015;40:14916–24.

[158] Javadian P, Zlotea C, Ghimbeu CM, Latroche M, Tensen TR. Hydrogen storage properties of nanoconfined LiBH$_4$-Mg$_2$NiH$_4$ reactive hydride composites. J Phys Chem C 2015;119:5819–26.

[159] Shao J, Xiao XZ, Fan XL, Huang X, Zhai B, Li SQ, et al. Enhanced hydrogen storage capacity and reversibility of LiBH$_4$ nanoconfined in the densified zeolite-templated carbon with high mechanical stability. Nano Energy 2015;5:244–55.

[160] Chong L, Zeng XQ, Ding WJ, Liu DJ, Zou JX. NaBH$_4$ in: graphene wrapper: significantly enhanced hydrogen storage capacity and regenerability through nanoencapsulation. Adv Mater 2015;27:5070–4.

[161] Xia GQ, Chen XW, Zhou CF, Zhang CF, Li D, Gu QF, et al. Nano-confined multi-synthesis of a Li-Mg-N-H nanocomposite towards low-temperature hydrogen storage with stable reversibility. J Mater Chem A 2015;3:12646–52.

[162] Wang XB, Xie LH, Huang KW, Lai ZP. A rationally designed amino-borane complex in a metal-organic framework: a novel reusable hydrogen storage and size-selective reduction material. Chem Commun 2015;51:7610–3.

[163] Yang YJ, Liu YF, Li Y, Zhang X, Guo MX, Pan HG. Towards the endothermic dehydrogenation of nanoconfined magnesium borohydride ammoniate. J Mater Chem A 2015;3:11057–65.

[164] Zhang LJ, Xia GL, Ge Y, Wang CY, Guo ZP, Li XG, et al. Ammonia borane confined by nitrogen-containing carbon nanotubes: enhanced dehydrogenation properties originating from synergetic catalysts and nanoconfinement. J Mater Chem A 2015;3:20494–9.

[165] Han M, Zhao Q, Zhu ZQ, Hu YX, Tao ZL, Chen J. The enhanced hydrogen storage of micro-nanostructured hybrids of Mg(BH$_4$)$_2$-carbon nanotubes. Nanoscale 2015;7:18305–11.

[166] Zlotea C, Oumellal Y, Hwang SJ, Ghimbeu CM, De Jongh PE, Latroche M. Ultrasmall MgH$_2$ nanoparticles embedded in an ordered microporous carbon exhibiting rapid hydrogen sorption kinetics. J Phys Chem C 2015;119:18091–8.

[167] Wang YT, Wan CB, Meng XH, Ju X. Improvement of the LiBH$_4$ hydrogen desorption by confinement in modified carbon nanotubes. J Alloy Compd 2015;645:112–6.

[168] Zhong RQ, Zou RQ, Nakagawa T, Janicke M, Semelsberger TA, Burrell AK, et al. Improved hydrogen release from ammonia-borane with ZIF-8. Inorg Chem 2012;51:2728–30.

[169] Kalidindi SB, Esken D, Fischer RA. B-N chemistry@ZIF-8: dehydrocoupling of dimethylamine borane at room temperature by size-confinement effects. Chem Eur J 2011;17:6594–7.

[170] Stavila V, Bhakta RK, Alam TM, Majzoub EH, Allendorf MD. Reversible hydrogen storage by NaAlH$_4$ confined within a titanium-functionalized MOF-74 (Mg) nanoreactor. ACS Nano 2012;6:9807–17.

[171] Bhakta RK, Herberg JL, Jacobs B, Highley A, Behrens Jr R, Ockwig NW, et al. Metal-organic frameworks as templates for nanoscale NaAlH$_4$. J Am Chem Soc 2009;131:13198–9.

[172] Zhang X, Liu YF, Pang YP, Gao MX, Pan HG. Significantly improved kinetics, reversibility and cycling stability for hydrogen storage in NaAlH$_4$ with the Ti-incorporated metal-organic framework MIL-125(Ti). J Mater Chem A 2014;2:1847–54.

[173] Sun W, Li S, Mao J, Guo Z, Liu H, Dou S, et al. Nanoconfinement of lithium borohydride in Cu-MOFs towards low temperature dehydrogenation. Dalton Trans 2011;40:5673–6.

[174] Shao J, Xiao XZ, Fan XL, Zhang LT, Li SQ, Ge HW, et al. Low-temperature reversible hydrogen storage properties of LiBH$_4$: a synergetic effect of nanoconfinement and nanocatalysis. J Phys Chem C 2014;118:11252–60.

[175] Fang ZZ, Wang P, Rufford TE, Kang XD, Lu GQ, Cheng HM. Kinetic and thermodynamic-based improvements of lithium borohydride incorporated into activated carbon. Acta Mater 2008;56:6257–63.

[176] Ngene P, van Zwienen M, de Jongh PE. Reversibility of the hydrogen desorption from LiBH$_4$: a synergetic effect of nanoconfinement and Ni addition. Chem Commun 2010;46:8201–3.

[177] Nielsen TK, Bösenberg U, Gosalawit R, Dornheim M, Cerenius Y, Besenbacher F, et al. A reversible nanoconfined chemical reaction. ACS Nano 2010;4:3903–8.

[178] Fichtner M. Nanoconfinement effects in energy storage materials. Phys Chem Chem Phys 2011;13:21186–95.

[179] Ghoufi A. Nanoconfined gases, liquids and liquid crystals in porous materials. Mol Simulat 2014;40:698–712.

[180] De Jongh PE, Allendorf M, Vajo JJ, Zlotea C. Nanoconfined light metal hydrides for reversible hydrogen storage. MRS Bull 2013;38:488–93.

[181] Jeon KJ, Moon HR, Ruminski AM, Jiang B, Kisielowski C, Bardhan R, et al. Air-stable magnesium nanocomposites provide rapid and high-capacity hydrogen storage without using heavy-metal catalysts. Nat Mater 2011;10:286–90.

[182] Himmelberger DW, Alden LR, Bluhm ME, Sneddon LG. Ammonia borane hydrogen release in ionic liquids. Inorg Chem 2009;48:9883–9.

[183] Doroodian A, Dengler JE, Genest A, Rösch N, Rieger B. Methylguanidinium borohydride: an ionic-liquid-based hydrogen-storage material. Angew Chem Int Ed 2010;49:1871–3.

[184] Chen WD, Huang ZG, Wu GT, He T, Li Z, Chen J, et al. Guanidinium octahydrotriborate: an ionic liquid with high hydrogen storage capacity. J Mater Chem A 2015;3:11411–6.

[185] Rekken BD, Carre-Burritt AE, Scott BL, Davis BL. N-substituted amine-borane ionic liquids as fluid phase, hydrogen storage materials. J Mater Chem A 2014;2:16507–15.

[186] Welton T. Room-temperature ionic liquids. Solvents for synthesis and catalysis. Chem Rev 1999;99:2071–84.

[187] Dupont J, de Souza RF, Suarez PAZ. Ionic liquid (molten salt) phase organometallic catalysis. Chem Rev 2002;102:3667–91.

[188] Sahler S, Konnerth H, Knoblauch N, Prechtl MHG. Hydrogen storage in amine boranes: ionic liquid supported thermal dehydrogenation of ethylene diamine bisborane. Int J Hydrogen Energy 2013;38:3283–90.

[189] Wright WRH, Berkeley ER, Alden LR, Baker RT, Sneddon LG. Transition metal catalysed ammonia-borane dehydrogenation in ionic liquids. Chem Commun 2011;47:3177–9.

[190] Mahato S, Banerjee B, Pugazhenthi G, Banerjee T. Optimization and quantum chemical predictions for the dehydrogenation kinetics of ammonia borane-ionic liquid mixtures. Int J Hydrogen Energy 2015;40:10390–400.

[191] Bluhm ME, Bradley MG, Butterick R, Kusari U, Sneddon LG. Amineborane-based chemical hydrogen storage: enhanced ammonia borane dehydrogenation in ionic liquids. J Am Chem Soc 2006;128:7748–9.

[192] Li X, Ma X, Shi F, Deng Y. Hydrogen generation from formic acid decomposition with a ruthenium catalyst promoted by functionalized ionic liquids. ChemSusChem 2010;3:71–4.

[193] Scholten JD, Prechtl MHG, Dupont J. Decomposition of formic acid catalysed by a phosphine-free ruthenium complex in a task-specific ionic liquid. ChemCatChem 2010;2:1265–70.

[194] Bhargava BL, Yasaka Y, Klein ML. Hydrogen evolution from formic acid in an ionic liquid solvent: a mechanistic study by ab Initio molecular dynamics. J Phys Chem B 2011;115:14136–40.

[195] Yasaka Y, Wakai C, Matubayasi N, Nakahara M. Controlling the equilibrium of formic acid with hydrogen and carbon dioxide using ionic liquid. J Phys Chem A 2010;114:3510–5.

[196] Yuan X, Sun G, Asakura H, Tanaka T, Chen X, Yuan Y, et al. Development of palladium surface-enriched heteronuclear Au–Pd nanoparticle dehalogenation catalysts in an ionic liquid. Chem Eur J 2013;19:1227–34.

[197] Prechtl MHG, Sahler S. Hydrogen storage using ionic liquid media. Curr Org Chem 2013;17:220–8.

[198] Zhang JS, Fisher TS, Ramachandran PV, Gore JP, Mudawar I. A review of heat transfer issues in hydrogen storage technologies. J Heat Transf 2005;127:1391–9.

[199] Aleksić P, Næss E. Experimental study of thermal effects in a hydrogen cryo-adsorption storage system. ASME Conf Proc 2009:603–10. IMECE2009-10593.

[200] Huang BL, McGaughey AJH, Kaviany M. Thermal conductivity of metal-organic framework 5 (MOF-5): Part I. Molecular dynamics simulations. Inter J Heat Mass Trans 2007;50:393–404.

[201] Murashov VV, White MA. Thermal properties of zeolites: effective thermal conductivity of dehydrated powdered zeolite 4A. Mater Chem Phys 2002;75:178–80.

[202] Ahluwalia RK, Peng HJK. On-board and off-board performance of hydrogen storage options for light-duty vehicles. Inter J Hydrogen Energy 2012;37:2891–910.

[203] Ren JW, Musyoka NM, Langmi HW, Swartbooi A, North BC, Mathe M. A more efficient way to shape metal-organic framework (MOF) powder materials for hydrogen storage applications. Int J Hydrogen Energy 2015;40:4617–22.

[204] Sánchez AR, Klein HP, Groll M. Expanded graphite as heat transfer matrix in metal hydride bed. Inter J Hydrogen Energy 2003;28:515–27.

[205] Purewal J, Liu DG, Sudik A, Veenstra M, Yang J, Maurer S, et al. Improved hydrogen storage and thermal conductivity in high-density MOF-5 composites. J Phys Chem C 2012;116:20199–212.

[206] Purewal JJ, Liu D, Yang J, Sudik A, Siegel DJ, Maurer S, et al. Increased volumetric hydrogen uptake of MOF-5 by powder densification. Int J Hydrogen Energy 2012;37:2723–7.

[207] Ren JW, North BC. Shaping porous materials for hydrogen storage applications: a review. J Technol Innov Renew Energy 2014;3:12–20.

[208] Akhtar F, Andersson L, Ogunwumi S, Hedin N, Bergström L. Structuring adsorbents and catalysts by processing of porous powders. J Eur Ceram Soc 2014;34:1643–66.

[209] Ren JW, Langmi HW, North BC, Mathe M. Review on processing of metal-organic framework (MOF) materials towards system integration for hydrogen storage. Int J Energy Res 2015;39:607–20.

[210] Frenot A, Chronakis IS. Polymer nanofibers assembled by electrospinning. Curr Opin Colloid Interface 2003;8:64–75.

[211] Zhang Y, Ouyang H, Lim CT, Ramakrishna S, Huang ZM. Electrospinning of gelatin fibers and gelatin/PCL composite fibrous scaffolds. J Biomed Mater Res B 2005;72:156–65.

[212] Sambaer W, Zatloukal M, Kimmer D. 3D modelling of filtration process via polyurethane nanofiber based nonwoven filters prepared by electrospinning process. Chem Eng Sci 2011;66:613–23.

[213] Yang H, Hong W, Dong I. A controlled biochemical release device with embedded nanofluidic channels. Appl Phys Lett 2012;100:153510.

[214] Persano L, Camposeo A, Tekmen C, Pisignano D. Industrial upscaling of electrospinning and applications of polymer nanofibers: a review. Macromol Mater Eng 2013;298:504–20.

[215] Li D, Xia Y. Electrospinning of nanofibers: reinventing the wheel. Adv Mater 2004;16:1151–70.

[216] Greiner A, Wendorff J. Electrospinning: a fascinating method for the preparation of ultrathin fibers. Angew Chem Int Ed 2007;46:5670–703.

[217] Luo CJ, Stoyanov SD, Stride E, Pelanb E, Edirisinghe M. Electrospinning versus fibre production methods: from specifics to technological convergence. Chem Soc Rev 2012;41:4708–35.

[218] Haji A, Nasouti K, Shoushtari AM, Kaflou A. Reversible hydrogen storage in electrospun composite nanofibers. In: Proceedings of the international conference nanomaterials: applications and properties; 2013. p. 2. 03NCNN05, 1–4.

[219] Bazilevsky AV, Yarin AL, Megaridis CM. Co-electrospinning of Core–Shell fibers using a single-nozzle technique. Langmuir 2007;23:2311–4.

[220] Im JS, Kwon O, Kim YH, Park SJ, Lee YS. The effect of embedded vanadium catalyst on activated electrospun

CNFs for hydrogen storage. Micro Meso Mater 2008;115:514—21.

[221] Im JS, Park SJ, Kim TJ, Kim YH, Lee YS. The study of controlling pore size on electrospun carbon nanofibers for hydrogen adsorption. J Colloid Interface Sci 2008;318:42—9.

[222] Im JS, Park SJ, Kim T, Lee YS. Hydrogen storage evaluation based on investigations of the catalytic properties of metal/metal oxides in electrospun carbon fibers. Int J Hydrogen Energy 2009;34:3382—8.

[223] Im JS, Park SJ, Lee YS. The metal-carbon-fluorine system for improving hydrogen storage by using metal and fluoride with different levels of electronegativity. Int J Hydrogen Energy 2009;34:1423—8.

[224] Xia GL, Li D, Chen XW, Tan YB, Tang ZW, Guo AP, et al. Carbon-coated Li_3N nanofibers for advanced hydrogen storage. Adv Mater 2013;25:6238—44.

[225] Kim K, Lee D, Moon J. Co-electrospun Pd-coated porous carbon nanofibers for hydrogen storage applications. Int J Hydrogen Energy 2011;36:3566—73.

[226] Shahgaldi S, Yaakob Z, Jalil NM, Tasirin SM. Synthesis of high-surface-area hexagonal $LaNi_5$ nanofibers via electrospinning. J Alloy Compd 2012;541:335—7.

[227] Ren J, Musyoka NM, Annamalai P, Langmi HW, North BC, Mathe M. Electrospun MOF nanofibers as hydrogen storage media. Int J Hydrogen Energy 2015;40:9382—7.

[228] Dennison DM. A note on the specific heat of the hydrogen molecule. Proc Roy Soc Ser A (London) 1927;115:483—6.

[229] (a)Fukutani K, Sugimoto. Physisorption and ortho-para conversion of molecular hydrogen on solid surfaces. Prog Surf Sci 2013;88:279—348.
(b)http://www.fluxindia.com/maxioxb2.html. [Access 24 June 2016].

[230] Matsumoto M, Espenson JH. Kinetics of the interconversion of parahydrogen and orthohydrogen catalyzed by paramagnetic complex Ions. J Am Chem Soc 2005;127:11447—53.

[231] Moore DT, Miller GE. Rotationally resolved infrared laser spectroscopy of $(H_2)_n$-HF and $(D_2)_n$-HF (n = 2—6) in helium nanodroplets. J Phys Chem A 2004;108:1930—7.

[232] Wakao N, Selwood PW, Smith JM. Low temperature ortho-para hydrogen conversion-kinetic studies. AIChE J 1962;8:478—81.

[233] Leachman JW, Jacobsen RT, Penoncello SG, Lemmon EW. Fundamental equations of state for parahydrogen, normal hydrogen, and orthohydrogen. J Phys Chem Ref Data 2009;38:721—48.

[234] Schmauch GE, Singleton AH. Technical aspects of ortho-parahydrogen conversion. Ind Eng Chem 1964;56:20—31.

[235] Kinard GE. The commercial use of liquid hydrogen over the last 40 years. In: Dew-Hughes D, Scurlock RG, Watson JHP, editors. Proceedings of the international cryogenic engineering conference. Bristol, UK: Institute of Physics; 1998. p. 39—44.

[236] McIntosh GE. Applications of ortho-para hydrogen catalyst. IOP Conf Ser 2015;101:012079. http://dx.doi.org/10.1088/1757-899X/101/1/012079.

[237] Buntkowsky G, Walaszek B, Adamczyk A, Xu Y, Limbach HH, Chaudret B. Mechanism of nuclear spin initiated para-H_2 to ortho-H_2 conversion. Phys Chem Chem Phys 2006;8:1929—35.

[238] Kosone T, Hori A, Nishibori E, Kubota Y, Mishima A, Ohba M, et al. Coordination nano-space as stage of hydrogen ortho-para conversion. R Soc Open Sci 2015;2:150006.

[239] Ao ZM, Hernández-Nieves AD, Peeters FM, Li S. The electric field as a novel switch for uptake/release of hydrogen for storage in nitrogen doped graphene. Phys Chem Chem Phys 2012;14:1463—7.

[240] Song NH, Wang YS, Gao HY, Jiang WF, Zhang J, Xu B, et al. Electric field improved hydrogen storage of Ca-decorated monolayer MoS_2. Phys Lett 2015;379:815—9.

[241] Tomaszewska A, Stępień ZM. The influenced of the external electric field on the hydrogen-palladium system. J Phys 2007;79:012028.

[242] Sun X, Huwang JY, Shi SZ. Hydrogen storage in mesoporous metal oxides with catalyst and external electric field. J Phys Chem C 2010;114:7178—84.

[243] Kim JH, Kang SW, Nah IW, Oh IH. Synthesis and characterization of Fe-modified zeolite for spin conversion of hydrogen at cryogenic temperature. Int J Hydrogen Energy 2015;40:15529—33.

[244] Kim JH, Karng SW, Oh IH, Nah IW. Ortho-para hydrogen conversion characteristics of amorphous and mesoporous Cr_2O_3 powders at a temperature of 77 K. Int J Hydrogen Energy 2015;40:14147—53.

[245] Das T, Kweon SC, Choi JG, Kim SY, Oh IH. Spin conversion of hydrogen over $LaFeO_3/Al_2O_3$ catalysts at low temperature: synthesis, characterization and activity. Int J Hydrogen Energy 2015;40:383—91.

[246] Zhang Z, Huang JY, Ning M, Li X. Field ionization effect on hydrogen adsorption over TiO_2-coated activated carbon. Int J Hydrogen Energy 2012;37:16018—24.

[247] Ubaid S, Xiao J, Zacharia R, Chahine R. Bénard. Effect of para-ortho conversion on hydrogen storage system performance. Int J Hydrogen Energy 2014;39:11651—60.

[248] Schlemminger C, Nœss E, Bünger U. Adsorption hydrogen storage at cryogenic temperature-material properties and hydrogen ortho-para conversion matters. Int J Hydrogen Energy 2015;40:6606—25.

[249] Terenzi C, Bouguet-Bonnet S, Canet D. Electron spin polarization transfer to ortho-H_2 by interaction of para-H_2 with paramagnetic species: a key to a novel para to ortho conversion mechanism. J Phys Chem Lett 2015;6:1611—5.

[250] Wagner S. Conversion rate of para-hydrogen to ortho-hydrogen by oxygen: implications for PHIP gas storage and utilization. Magn Reson Mater Phys 2014;27:195—9.

[251] Petitpas G, Aceves SM, Matthews MJ, Smith JR. Para-H_2 to ortho-H_2 conversion in a full-scale automotive cryogenic pressurized hydrogen storage up to 345 bar. Int J Hydrogen Energy 2014;39:6533—47.

[252] Peng JK, Ahluwalia PK. Enhanced dormancy due to para-to-ortho hydrogen conversion in insulated cryogenic pressure vessels for automotive applications. Int J Hydrogen Energy 2013;38:13664—72.

[253] Hövener JB, Bär S, Leupold J, Jenne K, Leibfritz D, Hennig J, et al. A continuous-flow, high-throughput, high-pressure parahydrogen converter for hyperpolarization in a clinical setting. NMR Biomed 2013;26:124—31.

[254] Svadlenak RE, Scott AB. The conversion of ortho-hydrogen to parahydrogen on iron oxide-zinc oxide catalysts. J Am Chem Soc 1957;79:5385—8.